Alaska Department of Transportation & Public Facilities
Alaska University Transportation Center

Cordova Floating Ferry Dock

Andrew T. Metzger, Ph.D., P.E.

December 2014

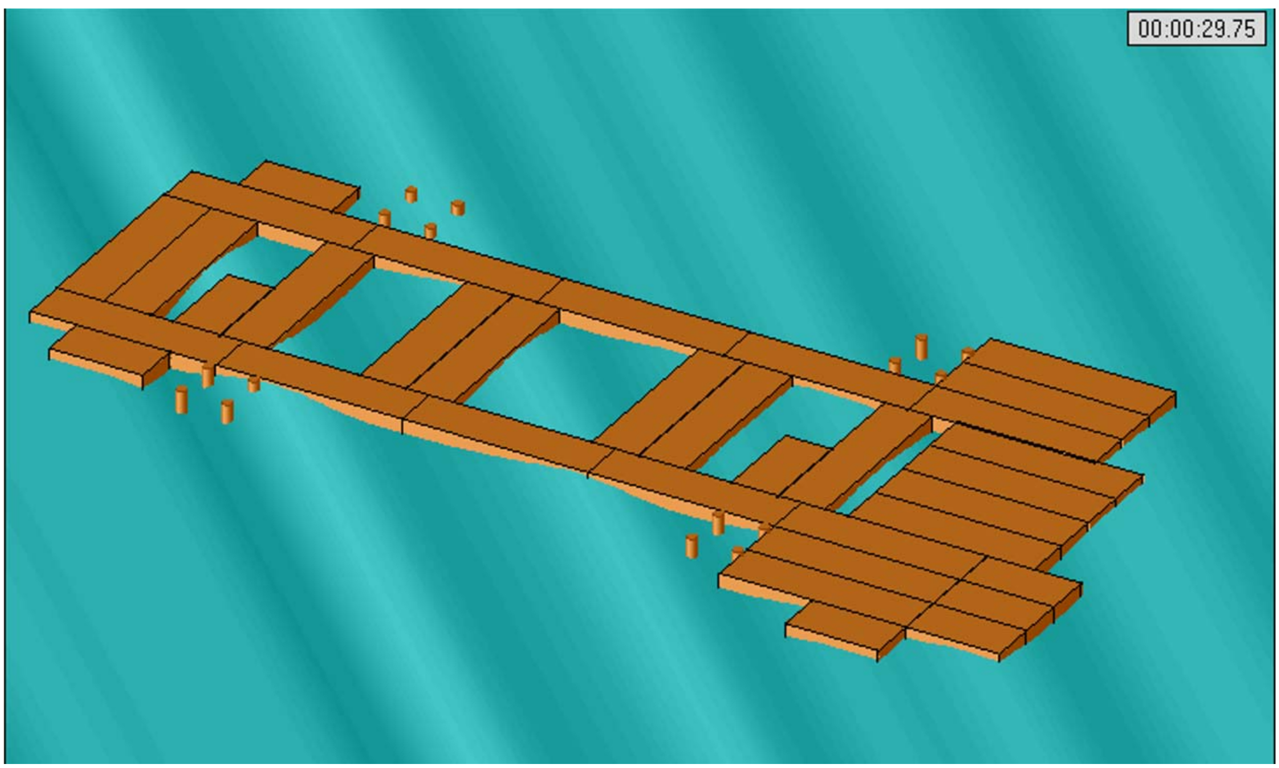

Alaska University Transportation Center
Duckering Building Room 245
P.O. Box 755900
Fairbanks, AK 99775-5900

Alaska Department of Transportation
Research, Development, and Technology Transfer
2301 Peger Road

INE/ AUTC 14.17

DOT&PF Report Number 4000(102)CB

Disclaimer

Notice

This document is disseminated under the sponsorship of the U.S. Department of Transportation in the interest of information exchange. The U.S. Government assumes no liability for the use of the information contained in this document. The U.S. Government does not endorse products or manufacturers. Trademarks or manufacturers' names appear in this report only because they are considered essential to the objective of the document.

Quality Assurance Statement

The Federal Highway Administration (FHWA) provides high-quality information to serve Government, industry, and the public in a manner that promotes public understanding. Standards and policies are used to ensure and maximize the quality, objectivity, utility, and integrity of its information. FHWA periodically reviews quality issues and adjusts its programs and processes to ensure continuous quality improvement.

Author's Disclaimer

Opinions and conclusions expressed or implied in the report are those of the authors. They are not necessarily those of the Alaska DOT&PF or funding agencies.

REPORT DOCUMENTATION PAGE			Form approved OMB No.
Public reporting for this collection of information is estimated to average 1 hour per response, including the time for reviewing instructions, searching existing data sources, gathering and maintaining the data needed, and completing and reviewing the collection of information. Send comments regarding this burden estimate or any other aspect of this collection of information, including suggestion for reducing this burden to Washington Headquarters Services, Directorate for Information Operations and Reports, 1215 Jefferson Davis Highway, Suite 1204, Arlington, VA 22202-4302, and to the Office of Management and Budget, Paperwork Reduction Project (0704-1833), Washington, DC 20503			
1. AGENCY USE ONLY (LEAVE BLANK) Report No. 4000(102)CB	2. REPORT DATE December 2014	3. REPORT TYPE AND DATES COVERED Final Report	
4. TITLE AND SUBTITLE Cordova Floating Ferry Dock			5. FUNDING NUMBERS Alaska DOT&PF AKSAS 4000(102)CB (T2-12-16)
6. AUTHOR(S) Andrew T. Metzger, Ph.D., P.E.			
7. PERFORMING ORGANIZATION NAME(S) AND ADDRESS(ES) Alaska University Transportation Center University of Alaska Fairbanks Duckering Building Room 245 P.O. Box 755900 Fairbanks, AK 99775-5900			8. PERFORMING ORGANIZATION REPORT NUMBER INE/AUTC 14.17
9. SPONSORING/MONITORING AGENCY NAME(S) AND ADDRESS(ES) State of Alaska, Alaska Dept. of Transportation and Public Facilities Research and Technology Transfer 2301 Peger Rd Fairbanks, AK 99709-5399			10. SPONSORING/MONITORING AGENCY REPORT NUMBER Report # 4000(102)CB
11. SUPPLENMENTARY NOTES			
12a. DISTRIBUTION / AVAILABILITY STATEMENT No restrictions			12b. DISTRIBUTION CODE
13. ABSTRACT (Maximum 200 words) This study began the evaluation of the Cordova floating ferry dock using the ANSYS AQWA software. The AQWA software models the effects of waves, wind and current on floating structures. Floating bodies are modeled as a point-mass with inertial and hydrostatic characteristics. As part of the study, the critical wave characteristic was defined. During the modeling it was found that AQWA can only model rigid bodies and that the Cordova floats experience a wide range of wave periods and directions. Consequently, AQWA requires adaptation to fully model the ferry dock at Cordova.			
14- KEYWORDS : Floating docks (Pmhbmpmff)			15. NUMBER OF PAGES 54
			16. PRICE CODE N/A
17. SECURITY CLASSIFICATION OF REPORT Unclassified	18. SECURITY CLASSIFICATION OF THIS PAGE Unclassified	19. SECURITY CLASSIFICATION OF ABSTRACT Unclassified	20. LIMITATION OF ABSTRACT N/A

NSN 7540-01-280-5500

STANDARD FORM 298 (Rev. 2-98)
Prescribed by ANSI Std. 239-18 298-1

SI* (MODERN METRIC) CONVERSION FACTORS

APPROXIMATE CONVERSIONS TO SI UNITS

Symbol	When You Know	Multiply By	To Find	Symbol
		LENGTH		
in	inches	25.4	millimeters	mm
ft	feet	0.305	meters	m
yd	yards	0.914	meters	m
mi	miles	1.61	kilometers	km
		AREA		
in^2	square inches	645.2	square millimeters	mm^2
ft^2	square feet	0.093	square meters	m^2
yd^2	square yard	0.836	square meters	m^2
ac	acres	0.405	hectares	ha
mi^2	square miles	2.59	square kilometers	km^2
		VOLUME		
fl oz	fluid ounces	29.57	milliliters	mL
gal	gallons	3.785	liters	L
ft^3	cubic feet	0.028	cubic meters	m^3
yd^3	cubic yards	0.765	cubic	m^3
		meters NOTE: volumes greater than 1000 L shall be		
		MASS		
oz	ounces	28.35	grams	g
lb	pounds	0.454	kilograms	kg
T	short tons (2000 lb)	0.907	megagrams (or "metric ton")	Mg (or "t")
		TEMPERATURE (exact degrees)		
^oF	Fahrenheit	5 (F-32)/9 or (F-32)/1.8	Celsius	^oC
		ILLUMINATION		
fc	foot-candles	10.76	lux	lx
fl	foot-Lamberts	3.426	candela/m^2	cd/m^2
		FORCE and PRESSURE or STRESS		
lbf	poundforce	4.45	newtons	N
lbf/in^2	poundforce per square inch	6.89	kilopascals	kPa

APPROXIMATE CONVERSIONS FROM SI UNITS

Symbol	When You Know	Multiply By	To Find	Symbol
		LENGTH		
mm	millimeters	0.039	inches	in
m	meters	3.28	feet	ft
m	meters	1.09	yards	yd
km	kilometers	0.621	miles	mi
		AREA		
mm^2	square millimeters	0.0016	square inches	in^2
m^2	square meters	10.764	square feet	ft^2
m^2	square meters	1.195	square yards	yd^2
ha	hectares	2.47	acres	ac
km^2	square kilometers	0.386	square miles	mi^2
		VOLUME		
mL	milliliters	0.034	fluid ounces	fl oz
L	liters	0.264	gallons	gal
m^3	cubic meters	35.314	cubic feet	ft^3
m^3	cubic meters	1.307	cubic yards	yd^3
		MASS		
g	grams	0.035	ounces	oz
kg	kilograms	2.202	pounds	lb
Mg (or "t")	megagrams (or "metric ton")	1.103	short tons (2000 lb)	T
		TEMPERATURE (exact degrees)		
^oC	Celsius	1.8C+32	Fahrenheit	^oF
		ILLUMINATION		
lx	lux	0.0929	foot-candles	fc
cd/m^2	candela/m^2	0.2919	foot-Lamberts	fl
		FORCE and PRESSURE or STRESS		
N	newtons	0.225	poundforce	lbf
kPa	kilopascals	0.145	poundforce per square inc h	lbf/in^2

*SI is the symbol for the International System of Units. Appropriate rounding should be made to comply with Section 4 of ASTM E380. (Revised March 2003)

ACKNOWLEDGMENTS

The author wish to acknowledge the technical support provided by the following:

- W. Seeling who help me with implementation of ANSYS AQWA software.
- Oceana Francis who provided the wave analysis and predictive data.

The author also acknowledges the funding provided by the Alaska Department of Transportation & Public Facilities and the assistance of the Alaska University Transportation Center.

Table of Contents

Project Synopsys

The Cordova Float study was authorized by AKDOT&PF to evaluate the behavior of the floating ferry dock at Cordova, Alaska. The purpose of the study was to gain further insight into the forces between the “floats” used to support the ferry landing structure. The system uses a number of pre-fabricated steel floats that are locked together to act as a support for the dock super structure. The methodology used in the project was to model the Cordova Float system using the ANSYS AQWA software.

ANSYS AQWA is an engineering analysis software for investigating the effects of waves, wind and current of floating structures. Floating bodies are modeled as a point-mass with inertial and hydrostatic characteristics of the actual body. The software has the ability to model wave diffraction off the body and realistically demonstrate its behavior when subjected to waves, currents, etc.

The development of the input variables can be found in Annex B. The following wave parameters with the probability of exceedance of $\leq$1% were developed:

Critical wave height, H1/100 = 2.5 meters,
Critical wave period, T1/100 = 6.8 seconds, and
Critical wave direction = 23°.

Preliminary results of the hydro dynamics for an individual float are in Annex A.

The Cordova Float assembly was modeled as shown in the Figure 1. The floats are locked together with very short/ stiff mooring line elements. The intent was to use the mooring line forces to estimated forces and bending moments between barges; in all six degrees of freedom.

During the initial analysis the following challenges or the use of AQWA were identified:

- Float Modeling: AQWA can only model rigid bodies (it is not an FEM software). However, the floats are not rigid (stiffness is not infinite) and accurate modeling will need to reflect this. Stiffness of the mooring line elements that connect the floats are input by the user and could be calibrated to reflect the stiffness of the floats being connected as well as the actual physical connecting hardware. This may require additional analysis of the floats as a shell structure (FEM analysis).
- The site of the Cordova Float is subject to a range of wave periods, propagating from a range of directions. Annex B can serve as a basis for estimating an envelope of wave periods and directions. Numerous analysis runs will have to be executed to determine the maximum design forces between floats. The number of runs could be pared down by considering predominate wave direction(s), but still using a range of wave periods.

These barriers must be overcome before a truly meaningful analysis can be completed. However, based on the limited runs completed, excessive pitch and roll at wave periods of about 3.1 seconds which is similar to the natural frequency of the pitch and roll.

At this point, it was decided not to continue with the next phase of the project due to the time, costs and uncertainties of overcoming the barriers noted. However, the information provided in Annex B provides useful information for future work on the Cordova harbor.

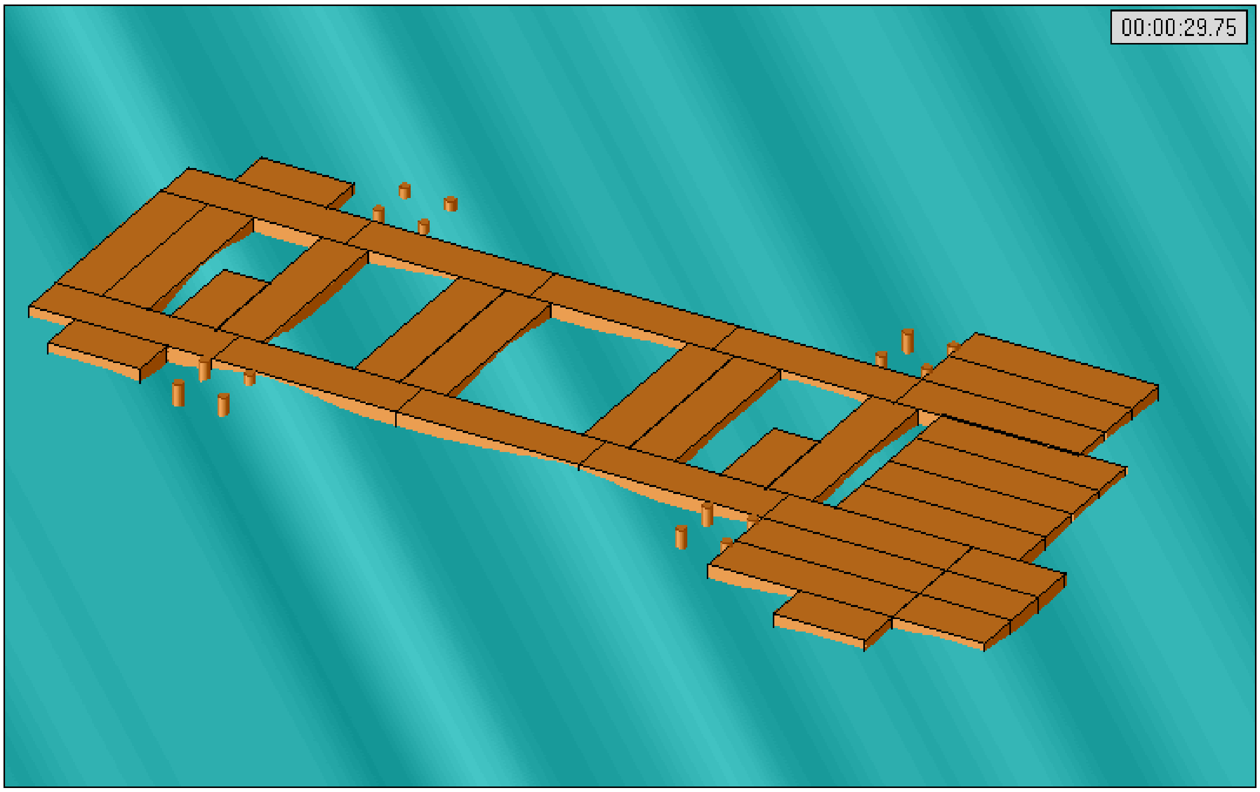

Figure 1. Cordova Float model subjected to wave conditions.

<u>ANNEX A</u>

Preliminary Analysis of Float System

Float 1

10’x20’x7’

Diffraction analysis

Panel size 0.2m sq; water depth 10m

Note:; similar to natural frequency in pitch and roll

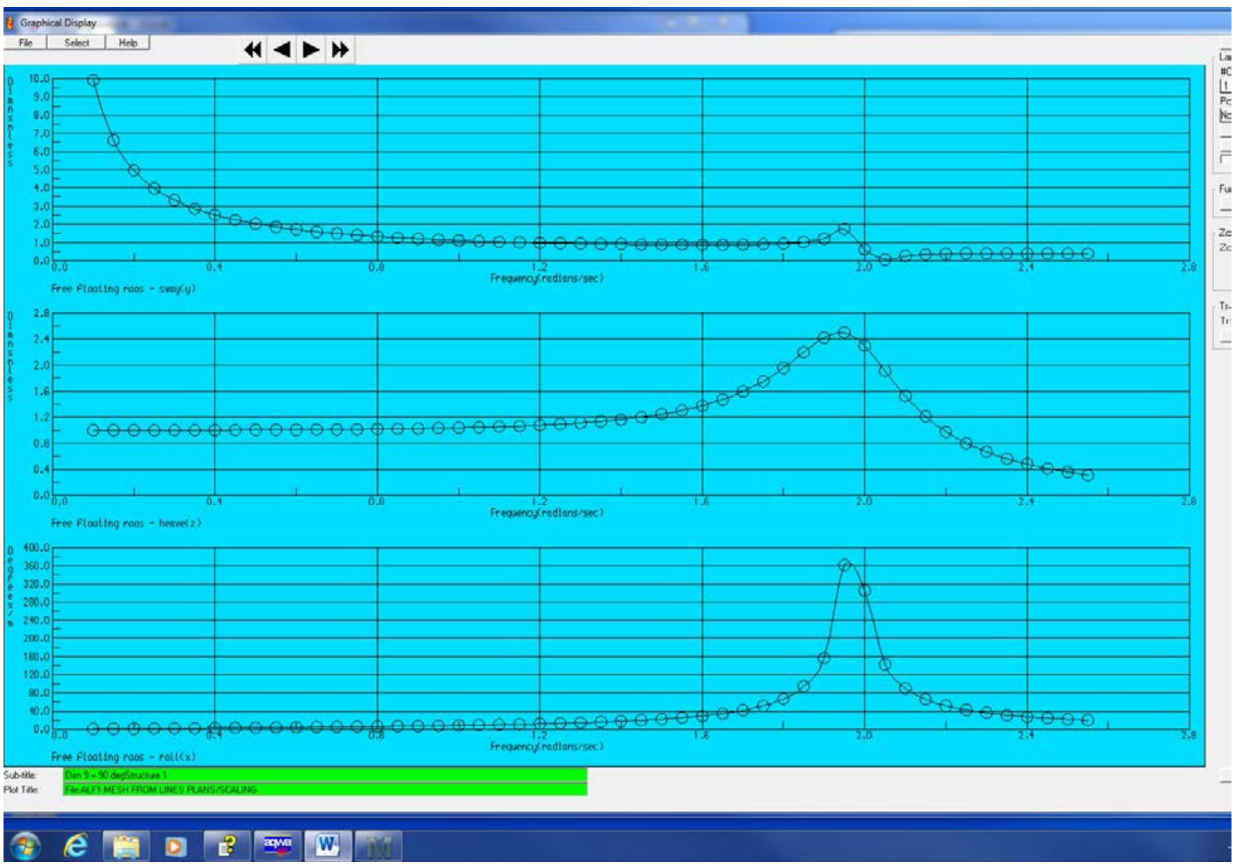

~doubled damping and run again:

Roll at 60deg with wave approach angle at 90deg

Doubled again and ran again:

End-on waves

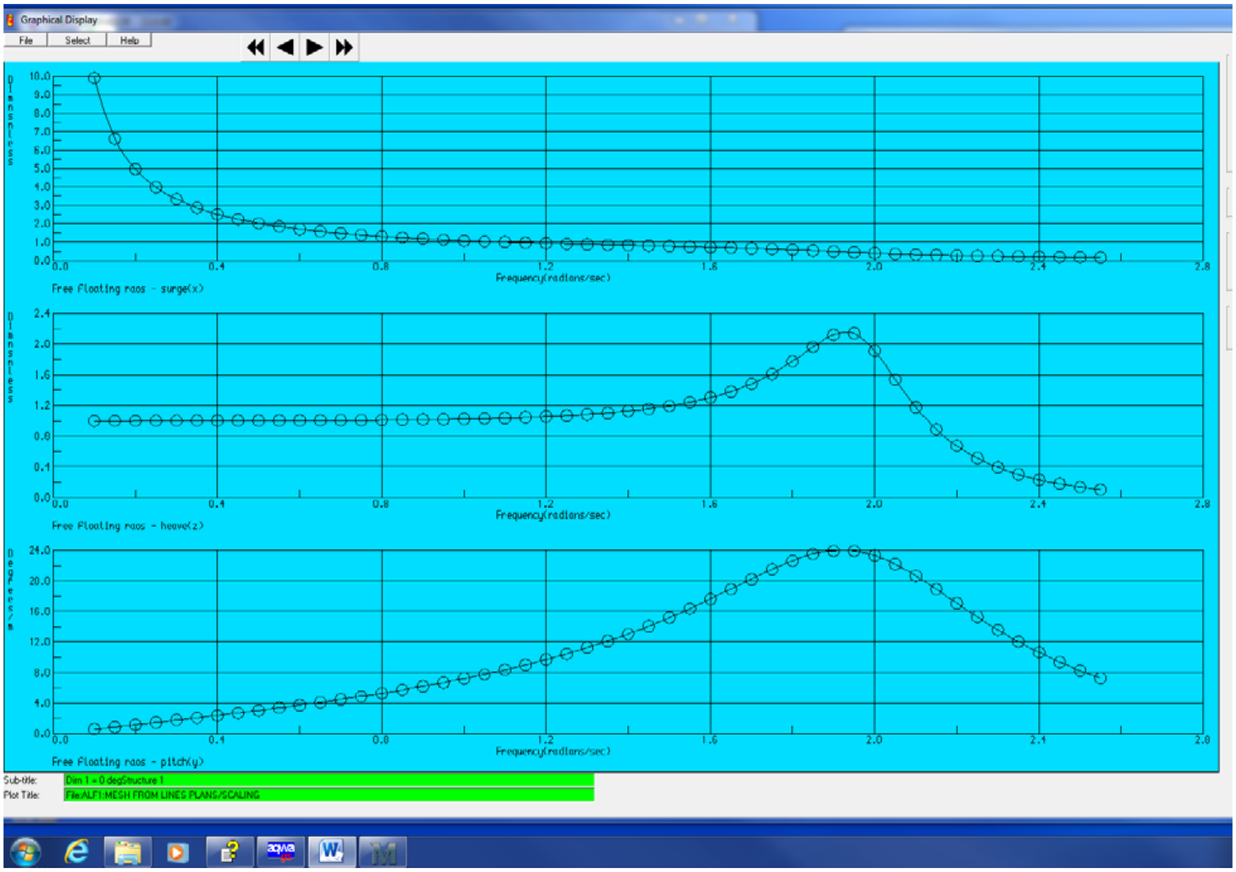

Broad-side waves

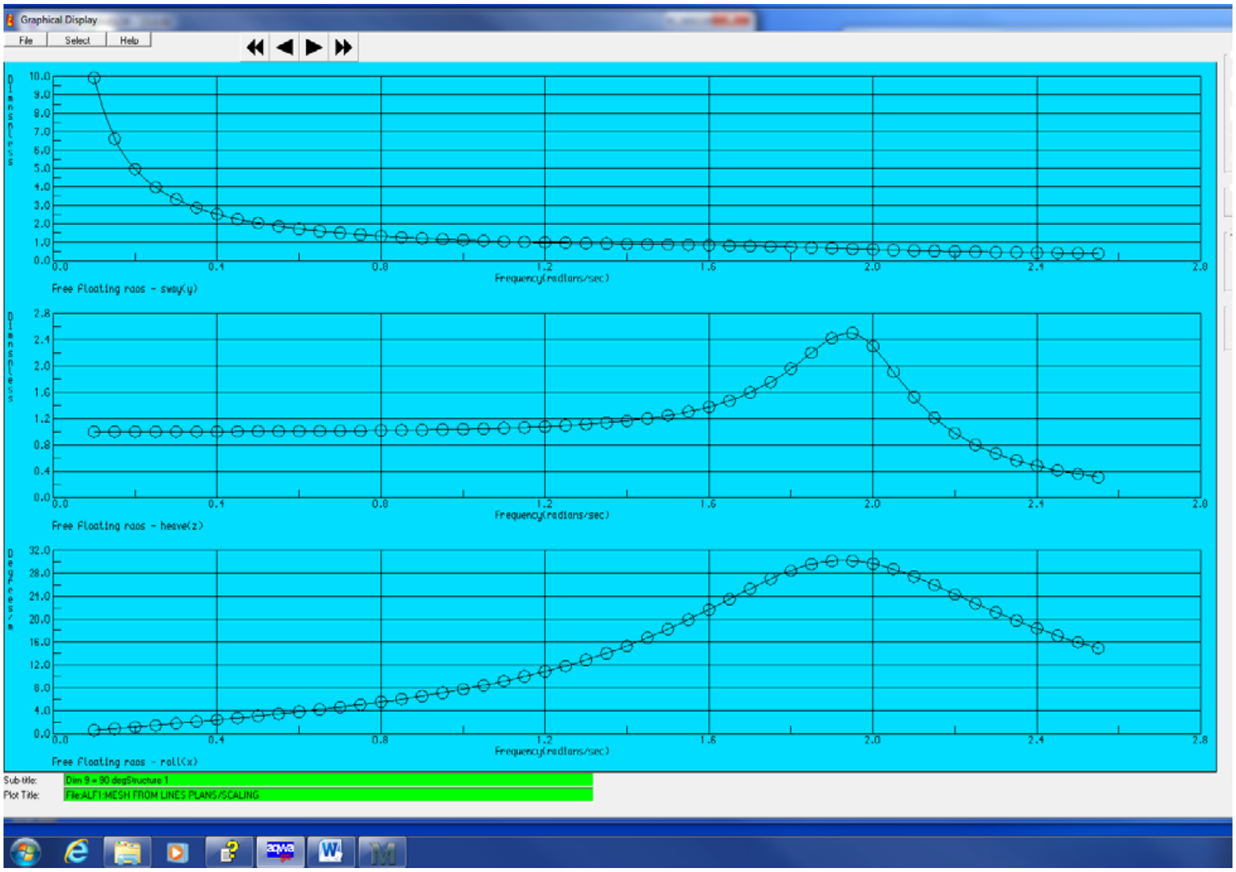

10X40 FLOAT

PLOTS WITH NO ADDED DAMPING

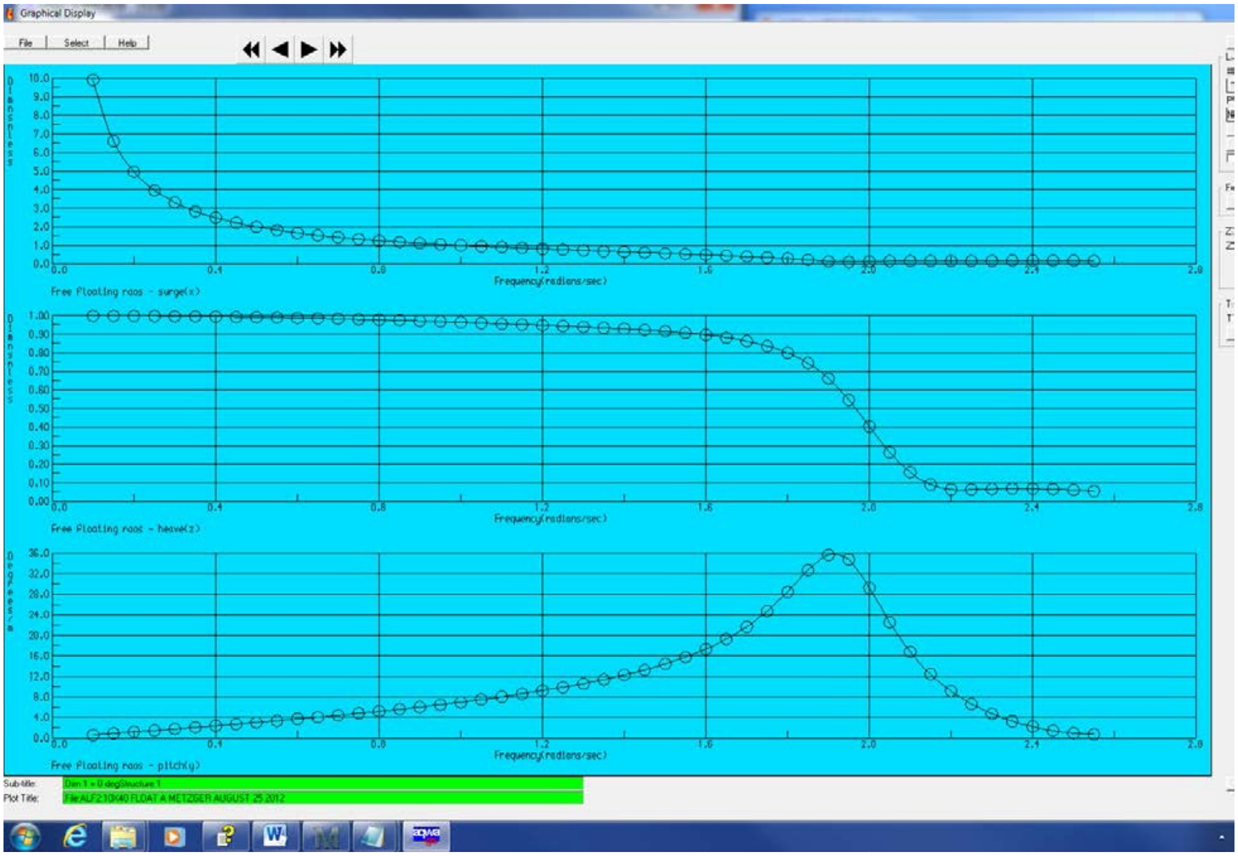

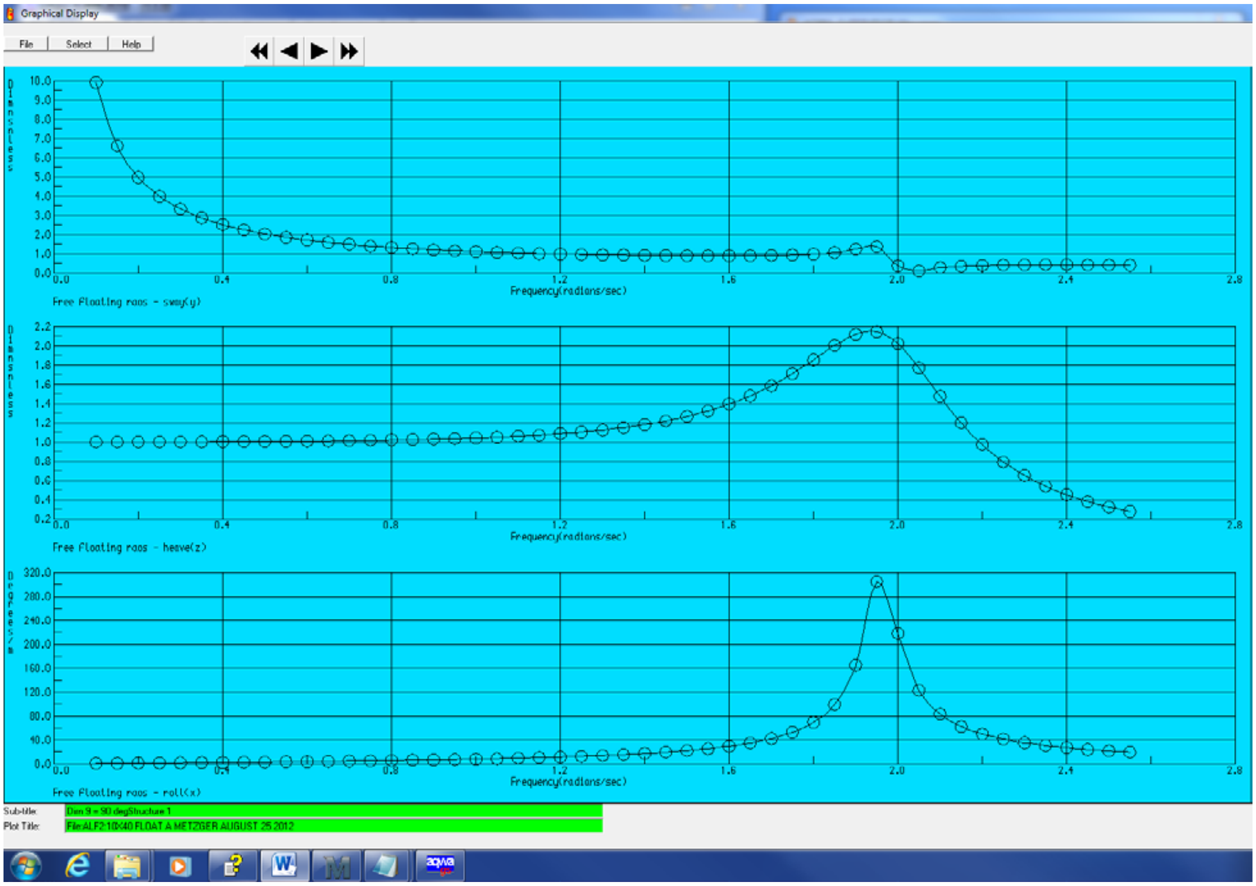
Graphical Display
File
Select
Help
Free Floating raos - sway(y)
Free Floating raos - heave(z)
Free Floating raos - roll(x)
Frequency(radians/sec)
Sub-title:
Plot Title:

ADDED DAMPING - ~4X DAMPING FROM DEFRACTION ANALYSIS

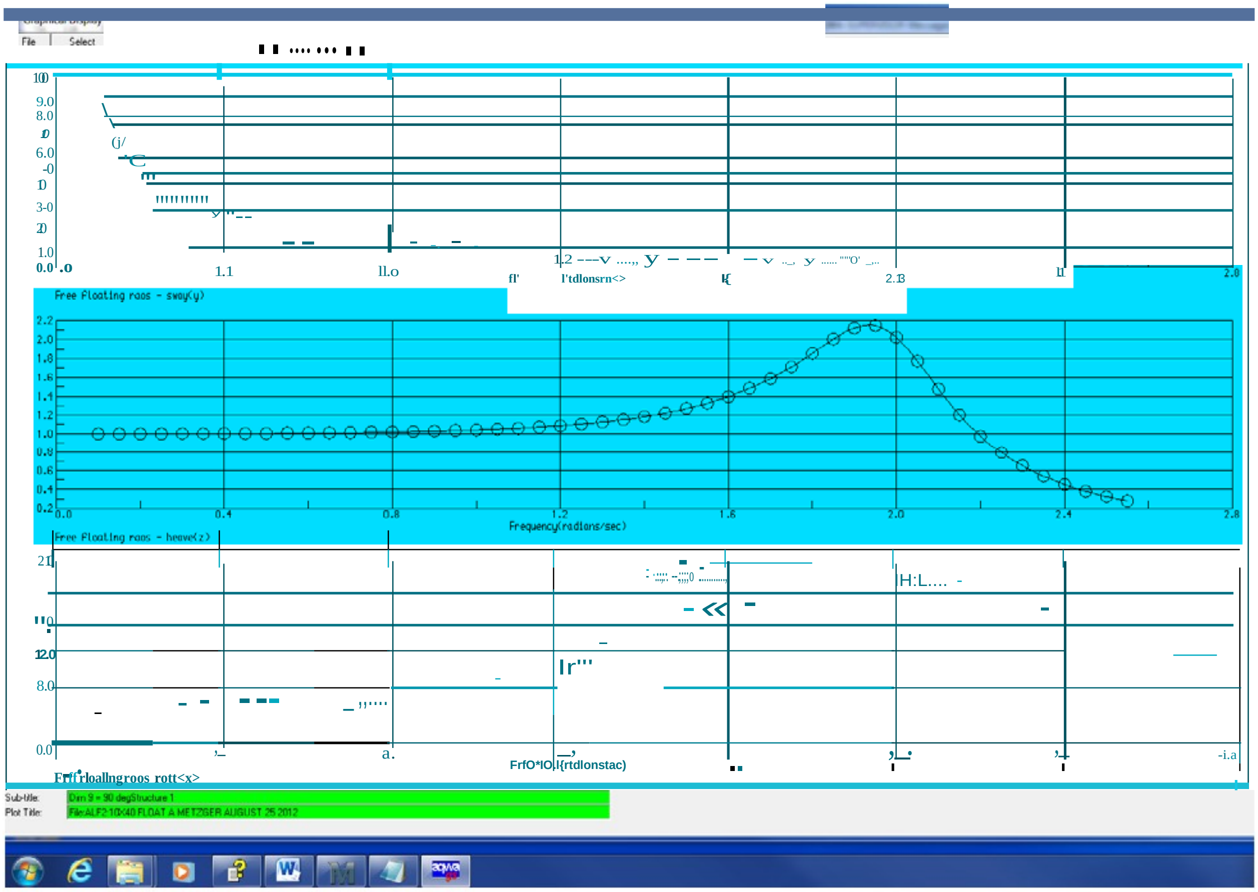

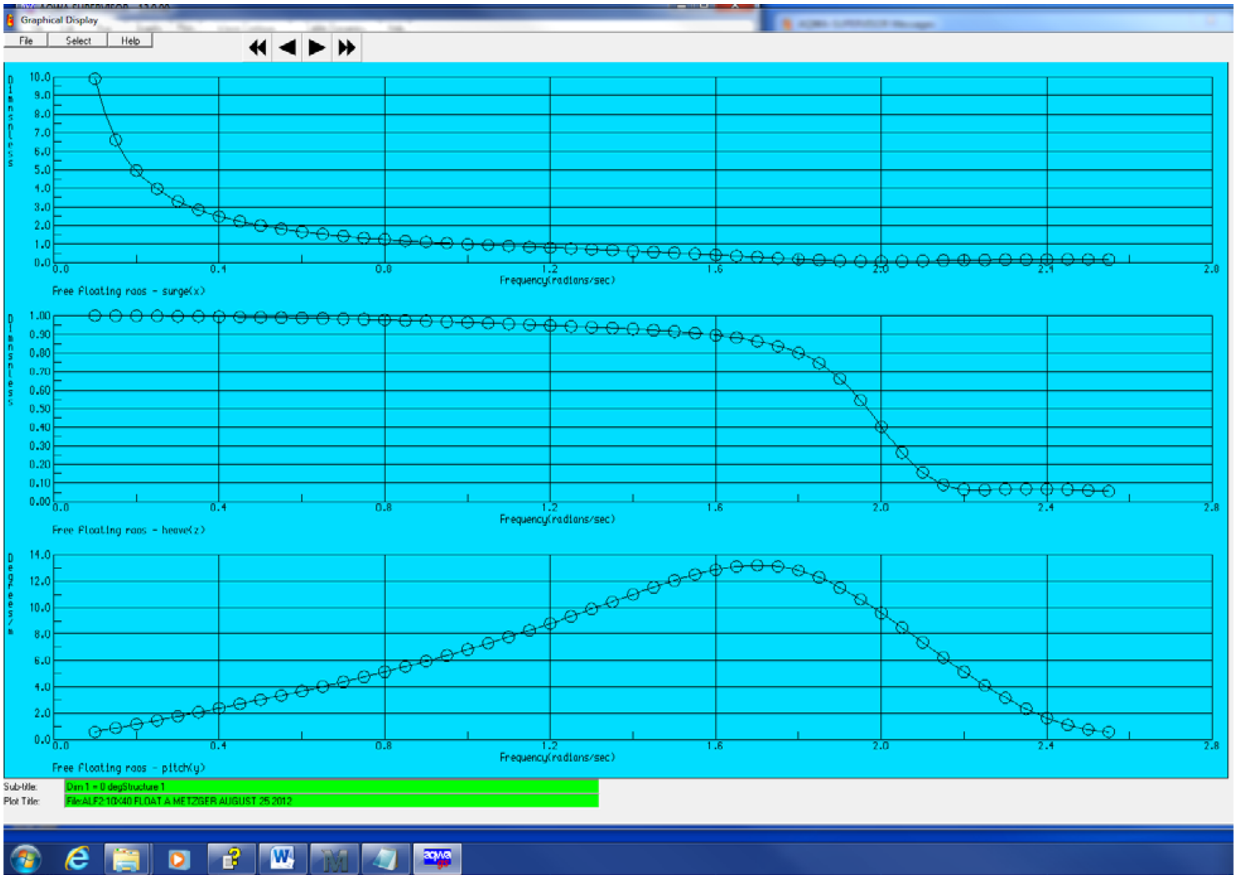
Graphical Display
File
Select
Help
Frequency(radians/sec)
Free Floating raos - surge(x)
Free Floating raos - heave(z)
Free Floating raos - pitch(y)
Sub-title:
Dim 1 = 0 degStructure 1
Plot Title:
File:ALF2 10X40 FLOAT A METZGER AUGUST 25 2012

ANNEX B – Report from Univ. of Hawaii

Design Wave Information for Cordova, Alaska

by

Oceana P. Francis, Ph.D., P.E.
Department of Civil & Environmental Engineering
University of Hawai'i at Mānoa
Honolulu, Hawaii 96822

August 31, 2013
Second Draft

Submitted to

Andrew Metzger, Ph.D., P.E.
Alaska University Transportation Center
Institute of Northern Engineering

Abstract

Being able to predict wave action is crucial to coastal communities. However, many things factor into wave action such as wind-wave energy transfer, wave breaking, and complex bathymetry among other. Hence to simplify calculations, shallow water fetch-limited wave equations were utilized. This was performed by using two different types of wave prediction methods (i.e. ACES and Bretschneider), Rayleigh's distribution method, and finite amplitude wave theory. The objective was to determine the most critical wave height/period/direction and the probability of exceedance at pile-guided floating ferry landings of a location lat 60.55718N, lon 145.75543W. From this study, the results yielded the following wave parameters with the probability of exceedence of $\leq$1%: Critical wave height, $H_{1/100}$ = 2.5 meters, Critical wave period, $T_{1/100}$ = 6.8 seconds, and Critical wave direction = 23°.

Table of Contents

Table of Figures

Table of Tables

1. Introduction

1.1. Background

The Alaska Marine Highway System (AMH) and the University of Alaska Fairbanks (UAF) needs design wave information for pile-guided floating ferry landings located in the Cordova, AK. Pile-guided floating ferry landings have distinct economic advantages, and AMS already has a number of these structures in service, including at the ferry terminal in Cordova, AK. These sectional barges “snap” together and is flexible in configuration as individual sections can be connected to provide a float with a desired configuration.

The region of study, Cordova, AK, is nestled near the mouth of the Copper River and at the head of Orca Inlet in eastern Prince William Sound (Figure 1 and Figure 2). Cordova is one of the few remaining finishing towns in Alaska, and with a heavy prevalence of about 800 boats and extensive fishing operations, it is one of state’s largest single basin harbors (City of Cordova, 2012).

The geographic area of Cordova encompasses approximately 61.4 square miles of land and 14.3 square miles of water. Population is estimated at about 2,240 as of 2009. Most land is now managed by the Chugach National Forest or by Eyak, a native Alaskan village corporation. In addition to its rich historical and cultural background, Cordova primarily focuses upon its fishing industry to survive. Half of all households have at least one person involved in commercial fishing or processing (CDFU, 2012).

Cordova’s geographic location generally protects itself from tsunamis from the Pacific Ocean (Chamberlin, 2011); however, the coastal regions of Cordova, Alaska can still be susceptible to tsunamis generated from earthquakes within the Alaska region, rising ocean levels, storm surges, and increasing wave heights. The closest deep-water passage to Cordova is through Prince

William Sound’s major 12-km-wide entrance, known as Hinchinbrook Entrance, 60 km west of the town. From the entrance, the route to Cordova passes east through deep Orca Bay, then through narrow (1 km wide) channels to the north of town.

To accurately describe the wave climate within the Orca Inlet, two different techniques can be employed. One is wave gaging and the other is wave hindcasting. Although a network of wave gages might eventually provide a good data source, the expense and time commitment that it would take was not possible. A viable alternative to wave gaging is to hindcast the wave climate using historical wind data. A variety of techniques are presently available to estimate water wave information from wind data. These methods are essentially models requiring computer solution or simple charts and formulas. The simplified, wind-generated, wave growth formulas within the Automated Coastal Engineering System (ACES, 1992) as developed by the Coastal Engineering Research Center of the Corps of Engineers was utilized as the wave hindcasting method in this project. The shallow-water formulations of ACES are based partly upon the fetch-limited, deep-water forms. The methods described in ACES are essentially those in Thompson and Vincent (1984), the Shore Protection Manual (SPM, 1984), and Smith (1991), but updated to included the latest field data for calibration of the semi-theoretical, wave growth formulas.

The pile-guided floating ferry landings are located at latitude 60deg 33.431min N (i.e. 60.55718), and longitude 145deg 45.326min W (i.e. 145.75543W = 214.24457E). Within this region, there is only one usable land-based wind station which is located at 60.557N 145.755W (i.e. at the pile-guided floating ferry landings) (NOAA, 2012a). However, there are a couple of limitations to this wind station. The first is that wind data only covers from 2010-2013. This is less than 3 years which is much too short a time period to do a complete wave hindcast which requires at least 20 years of data. The second is that there is only one land-based wind station found in this region. This would generally not be a good source to locate where the wind is generated at, but since the region of study is highly fetch-limited, the one land-based station gives a decent approximation.

Satellite gridded wind fields “North American Regional Reanalysis (NARR)” dataset (Mesinger et al. 2006) were used to understand the larger wind field in this region. Although, NARR was unable to cover the region of study because the resolution was too low, NARR was able to give a good synoptic and meso-scale understanding of the wind field in this region. The dataset covers 1979-2012 (i.e. 33 years) at a resolution of 0.3° or 1° which is taken from data-assimilative fluid-dynamic model. This system, a “reanalysis” data set, was developed and is maintained by the National Centers for Environmental Prediction (NCEP) of the US National Oceanic and Atmospheric Administration (NOAA).

From the wind data, the wave form can be classified, and the most critical wave height/period/direction and the probability of exceedance given. The critical wave height is not the significant wave height. The critical wave height may seldom be exceeded, and it is comparable with the highest 1% wave height (PIANC, 1992).

1.2. Objective

The objective of this study is to determine the most critical wave height/period/direction and the probability of exceedance at the pile-guided floating ferry landings (60.55718N, 145.75543W). This was performed by using two different types of wave prediction methods (i.e. ACES and Bretschneider), and using Rayleigh’s distribution to estimate probability of exceedance. Also, commentary on the type of wave form is included.

2. Methodology

2.1. Background

Hindcasting wind-waves in coastal and fetch-limited areas has been performed by reducing the spectral shapes into formulas and nomographs for wind-wave hindcasting purposes. Wave characteristics (height and period) are determined from three wind parameters (speed, duration and fetch distance) and have been modified to include depth-limiting effects (i.e., dissipation) for shallow and transitional water. These formulas are essentially one-dimensional estimates for wave characteristics along a dominant fetch direction and directional spreading of wave energy which is implicitly included in the formulations. The wave-hindcast formulas as specified in the SPM (1984) and as incorporated and refined within the ACES (Version 4.03) software package are employed for this project. The waves are characterized by significant wave height, H_{m0} and the peak spectral period, T_P.

2.2. ACES 4.03

The methodologies represented in the latest formulation (Version 4.03) of ACES provide quick and simple estimates for wave growth over open-water and restricted fetches in deep and shallow water. Wind-waves grow as a result of a flux of momentum and energy from the air above the waves into the wave field.

The frictional effects due to the presence of the water and the land surface distort the wind field thus, wind speed and direction become dependent upon elevation above the mean surface, roughness of the surface, air-sea temperature difference, and horizontal temperature gradients.

All wave conditions generated assume constant water depths over the wind duration, therefore, changes in the water elevation caused by the tides during the wind event are neglected.

The wave growth formulation used in this study is classified into a shallow-water form with complex, limiting geometry designated with restricted fetch conditions.

The restricted fetch methodology applies the concept of wave development in off-wind directions and considers the shape of the basin. Radial fetch lengths and angles measured from the point of interest are used to describe the geometry of the basin. The conventions used for specifying wind direction and fetch geometry are illustrated in Figure 3.

The assumptions and limitations regarding the use of the simplified ACES (4.03) model include: energy from the presence of other existing wave trains (e.g. ocean swell) is neglected, relatively short fetch geometry, relatively constant wind speed and direction, neutral stability condition, fixed value of drag coefficient, nearshore wave transformations are not considered, depth-induced wave breaking and surf zone process are not defined.

The approach wind direction, as well as the first radial fetch angle, and the radial fetch increment, are specified in a clockwise direction from north at the point of interest where, wave growth prediction is required.

Hindcasting procedures are as follows for the restricted fetch method:

1. Select a point of interest
2. Define the longest fetch length and direction from all possible directions
3. Input the wind direction from the longest fetch direction
4. Compute mean water depth along the longest fetch by the weighted-average method
5. Measure radial fetch lengths and angles to describe the geometry of the basin
6. Input all data into ACES

2.3. Bretschneider Nomogram

Surface ocean waves are produced by winds. The height of these waves depends upon wind speed, the length of time the wind blows (duration) and the distance over which the wind blows (fetch). In 1952, Charles Bretschneider (1952) created a diagram for wave prediction produced by specific wind conditions. Figure 4 (Bretschneider, 1970) shows this diagram (i.e. “Bretschneider Nomogram”). The *y*-axis shows wind speed, the *x*-axis describes fetch, the solid curved lines in the middle of the diagram show the wave height and wave period, and the slanted dashed lines represent wind duration.

2.4. Rayleigh Distribution

The Rayleigh distribution is used to generally plot a wave record from high wind event. The wave record is then analyzed to determine the individual wave heights and the results are plotted as height versus frequency distribution. This would typically yield the distribution shown where p(H) is the frequency or probability of the occurrence of the wave height H. Longuet-Higgins (1952) demonstrated that a Rayleigh distribution best defines the distribution of wave heights in a storm, and the following is taken from Sorenson (1993).

For design purposes, it would be extremely valuable to have a model for the distribution that applies to storm-generated waves. Therefore, other descriptive wave heights are often used. The root-mean-square height is

$$H_{rms} = \sqrt{\frac{\sum H_i^2}{N}} \tag{1}$$

where H_i are the individual wave heights in a record containing N waves. And in a manner similar to the significant wave height, we can define a height H_n, which represents the average of the highest *n* percent of waves. Thus, the significant wave height $H_{1/3}$ (or H_{m0}) is the average height of the shaded upper third of the wave heights. The mean of the highest one-tenth of all waves in a wave sample is denoted as $H_{1/10}$. The mean of the highest one-hundredth of all waves in a wave sample is denoted as $H_{1/100}$.

By knowing a representative wave height such as $H_{1/3}$ or H_{rms}, one could estimate any H_n and the percentage of waves that would exceed this H_n value. Therefore, the Rayleigh distribution takes the form of

$$p(H) = \frac{2H}{(H_{rms})^2} \exp\left[-\left(\frac{H}{H_{rms}} \right)^2 \right] \tag{2}$$

where H_{rms} is used to give a base magnitude to the distribution. The cumulative probability distribution *P(H)* (i.e. the percentage of waves having a height equal to or less than *H*) is given by

$$P(H) = 1 - \exp\left[-\left(\frac{H}{H_{rms}} \right)^2 \right] \tag{3}$$

The probability of exceedence is the percentage of waves having a height greater than a given height, which is of most interest for engineering design purposes is

$$Q(H) = 1 - P(H) = \exp\left[-\left(\frac{H}{H_{rms}} \right)^2 \right] \tag{4}$$

Thus, *Q(H)* represents the area under the *p(H)* versus *H* curve to the right of the given *H* value.

2.5. Wave Theory

2.5.1 Finite amplitude wave theory

Due to the nature of the wind-wave interaction in the enclosed inlet, the simplest of phase-resolving models was applied. Phase-resolving models are fully deterministic models based on hydrodynamics conservation laws, i.e. conservation of mass, momentum and energy (Losada and Revilla, 2009).

Finite amplitude wave theory was first developed by Airy (1845) and Stokes (1847). Solving and understanding Stokes' equations means laying out the basis of Airy wave equations. The Airy wave theory satisfactorily explains ~90% of all wave analysis situations and is in fact used for most engineering purposes.

Sorensen (1993) gives the general expression for water surface elevation (η) as

$$\eta = a\cos(\theta) + a^2 B_2(L,d)\cos(2\theta) + a^3 B_3(L,d)\cos(3\theta) + ...a^n B_n(L,d)\cos(n\theta) \qquad (5)$$

where a is the wave amplitude (m), θ is the phase function (radians), L is the wavelength (m), d is the depth (m), and B is a non-constant variable.

Airy (Linear) wave theory is based on the assumption that the wave amplitude is small and the contribution made to the solution by higher order terms in Equation 5 is negligible. Therefore, the Airy wave equations (Airy, 1845) is solved for the water surface elevation (η_1), which is characterized by a sinusoidal waveform of wavelength L, height H and period T. The symbols x denotes the horizontal displacement of the water surface relative to the stillwater level, t denotes time, and the amplitude of the wave a is one-half of the wave height H and is given in the U.S Army *Shore Protection Manual*, (SPM, 1984) as

$$\eta_1 = \frac{H}{2}\cos 2\pi\left(\frac{x}{L_1} - \frac{t}{T}\right) \qquad (6)$$

where the wavelength L_1 for the first-order theory is

$$L_1 = \frac{gT^2}{2\pi} \tanh\left(\frac{2\pi d}{L_1}\right) \tag{7}$$

where d is the depth (m).

2.5.2 Higher order wave theory

For situations where wave steepness departs from a sinusoidal form, i.e., exhibiting increased steepness, higher-order wave theories are more appropriate; examples include Stokes (second-, third-, and fifth-order) and Cnoidal. Stokes (1847) second-order wave theory states that H/d not to be large, therefore is applicable for deep water and most intermediate depth range.

From Equation 6, $a = H/2$, for first (Airy) and second (Stokes 2nd) orders, and B^2, B^3 are specified functions of the wavelength L and depth d. Therefore, the water surface elevation, η_2 for second-order theory (Stokes, 1847) as referenced in the U.S Army *Shore Protection Manual* (SPM, 1984) would be the following, where all the variable are defined above

$$\eta_2 = \frac{H}{2}\cos 2\pi\left(\frac{x}{L} - \frac{t}{T}\right) + \frac{\pi H}{8}\left(\frac{H}{L}\right)\frac{\cosh(2\pi d/L)}{\sinh^3(2\pi d/L)}\left[2 + \cosh(4\pi d/L)\right]\cos 4\pi\left(\frac{x}{L} - \frac{t}{T}\right) \tag{8}$$

The wavelength (L_2) for second-order theory is identical to those obtained by first-order linear theory. Therefore, second-order theory (Stokes, 1847) wavelength, L_2, as shown in the U.S Army *Shore Protection Manual*, (SPM, 1984) is:

$$L_2 = \frac{gT^2}{2\pi} \tanh\left(\frac{2\pi d}{L_2}\right) \tag{9}$$

3. Data and Description

Wind data was derived from three sources which were: North American Regional Reanalysis (Mesinger et al. 2006), Bretschneider Nomogram (Bretschneider, 1970), and National Buoy Data Center (NOAA, 2012a). The data and analysis of each are described here in this section.

The Merle K. (Mudhole) Smith Airport (Cordova's Airport) was considered for wind data but was dismissed as a data source. Wind records examined at Cordova airport indicate a strong easterly direction (Diebel and Norda, 2013), however the fetch length measured in this study to the east of Station CRVA2 was << 1km (Table 1), so only the north-easterly direction affects Station CRVA2. This is due to the differing coastal (CRVA2) versus inland (Cordova Airport) locations and the mountains surrounding these stations.

3.1. Large gridded wind fields Elev.=111m

North American Regional Reanalysis (NARR) gridded wind data (Mesinger et al. 2006) at 0.3° resolution was considered for use in this project. However, since one degree of latitude equals 60 nautical miles (nm), and the longest fetch considered 6.54 nm, a 0.3° resolution for gridded wind field was considered too coarse a resolution for this enclosed bay. Although the distance between degrees of longitude isn't constant because they converge towards the poles, latitude is mainly being considered here because of fetch orientation. Therefore, NARR was used to evaluate overall vector winds over the Northern Gulf of Alaska to understand broader synoptic scale winds.

Synoptic-scale low-pressure systems over the Gulf of Alaska have associated winds which blow counterclockwise (the coast to the right of the direction of the wind) (Figure 5). Storms entering the Gulf follow two predominant pathways. One pathway is a west – east track across the Alaska Peninsula from the Bering Sea. The other is a southwest – northeast track across the Gulf of Alaska. The North American Regional Reanalysis (NARR) (Figure 5) gridded wind fields at a 1.0° resolution at the 925mb level (i.e. 762 m height) showed the predominant wind direction east-southeasterly with an associated average wind speed of approximately 21 m/s during 1979 to 2012 (33 years) just southeast of Cordova.

Mesoscale (30-100 km) variations especially affect the wind-wave channeling influence through straits and the mouths of bays and fjords (Spies, 2007). Orographic effects, especially in the winter, enhance mesoscale winds where continental air comes across the shelf and collides with marine air. These offshore-directed gap winds at the mouths of coastal embayments such as Hinchinbrook Entrance have been previously documented (Mackline et al., 1988).

At the pile-guided floating ferry landings in Cordova, the North American Regional Reanalysis (NARR) (Figure 6) gridded wind fields at a 0.3° resolution at the 1000mb level (i.e. 111m height) showed the predominant wind direction east-southeasterly with an associated wind speed of 13 m/s during 1979 to 2012 (33 years). Southeast of Cordova in the Gulf of Alaska the wind speeds averaged 16 m/s during 1979 to 2012 (33 years).

The results of NARR showed that these larger scale winds do not affect Station CRVA2 due to the surrounding fetch to the east and southeast, where fetch length <<1km and is surrounded by land. Therefore, wind stations located within the closed embayment, not outside of the embayment, must be used to accurately describe the wave action for this study.

3.2. <u>Single land-based wind station Elev.=12.5m</u>

Station CRVA2 is owned and maintained by NOAA's National Ocean Service (NOAA, 2012a). It is at the approximate lat and long of the pile-guided floating ferry landings. It is the only coastal wind station located within this closed embayment. The following parameters apply for this buoy:

- 60.557 N 145.755 W (60°33'27" N 145°45'19" W)
- Site elevation: 12.5 m above mean sea level
- Output (of interest): Wind magnitude and direction; No wave information
- Date: 2010-present

The station contains wind data at an hourly interval. The air-sea temperature difference was used in the ACES wind prediction.

There were 3 years of wind data: mean wind direction, wind speed, and gusts in 6-minute intervals. Only observations of wind speeds => 9 m/s were considered. Therefore, only the years 2010 and 2011 were considered. The year 2012 gave an unusually low wind speeds, where the highest was 9.9 m/s therefore this year was not considered.

The year 2010 (Figure 7), showed 551 observations of wind speeds => 9 m/s with an average wind speed of 11 m/s, wind direction of 39°, and an associated wind gust of 17 m/s. The highest wind speed reached 17.6 m/s, and wind direction 19°. Wind gust reached 31 m/s with an associated wind direction of 138°.

The year 2011 (Figure 8), showed 1400 observations of wind speeds => 9 m/s with an average wind speed of 11 m/s, wind direction of 50°, and an associated wind gust of 18 m/s. The highest wind speed reached 18.2 m/s, and wind direction 24°. Wind gust reached 36 m/s with an associated wind direction of 28°.

Station CRVA2 datasets (NOAA, 2012a) showed that all observations => 9 m/s considered fell between 0-90°, with largest amount observations and highest wind speeds out of the northeasterly direction, and the range between 36°-90° was enclosed by shoreline. For 2011, there were only 47 observations between 91-354°, and no observations between 177-270°. For 2010, there were only 6 observations between 91-354°. Table 1 shows the summary result for Station CRVA2 for 2011.

3.3. Wind duration from Bretschneider Nomogram

The Bretschneider Nomogram (Bretschneider, 1970) was used to approximate the wind duration based on wind speed and fetch length (Figure 4). From Station CRVA2 wind data for 2011, the Nomogram resulted in a 1.5-hour duration. This 1.5-hour duration was then entered into ACES.

The Bretschneider Nomogram was also used to estimate waves based on wind fetch. This is discussed later in this study.

3.4. Bathymetry from Hydrographic Surveys

All bathymetry data is from NOAA (NOAA, 2012b). NOAA has a user-friendly interaction map that shows all the hydrographic surveys within the database. A smaller scale NOAA Nautical Chart, Catalog No. 16710, Mercator Projection Scale 1:30,000, NAD 83, "Orca Bay and Inlet, Channel Islands to Cordova", Edition 18, Edition date: November 2010, was able to capture the bathymetry of the major fetch locations used in this report (i.e. Figure 3). A larger scale NOAA Nautical Chart, Catalog No. 16709, Mercator Projection Scale 1:80,000, NAD 83, "Prince William Sound, Eastern Entrance", Edition 25, Edition date: March 2011, was able to capture bathymetry for any remaining fetch in the far northern region of the Inlet, and the bathymetry southwest of Station CRVA2. Along the 24° fetch covering 6.54 nautical miles (12.1 km), there were three different sections roughly equal in distance, but where the bathymetry differed. Therefore, the weighted-average method was used. This included a section from Cordova to Observation Island with a depth of approximately 12 meters. Then the second section from Observation Island to North Island, the depth significantly decreases to about 3 meters. Then the third section from North Island to the beginning of the fetch length over Nelson Bay is about 30 meters. Averaging the fetch across these roughly equal distances averages to 15 meters. Along the 36° fetch covering only 0.52 nautical miles (0.97 km) the depth averaged 9 meters.

Since the 24° fetch was the wind direction of choice, a bathymetry of 15 meters was used for all calculations in this report.

4. Results and Discussion

4.1. Result 1 - ACES

Fetch results measured from Figure 3 were implemented into ACES and the results are given in Figure 9. Wind data from station CRVA2 for the calendar year 2011 was used for input, since it was the highest of all years between 2010-2012 that had recorded measurements.

Windspeed adjustment and wave growth were computed in ACES. Parameters included the type of wind fetch which was considered to be "shallow restricted". The average depth assumed was 15 m (NOAA, 2012b). The wind duration was assumed for 1.5 hours.

In ACES, 8 fetch lengths were entered with a radial angle increment of 12° (Table 1). This was based on wind observations for wind speeds => 9 m/s (Figure 8). The wind speed and direction entered was 18.2 m/s at 24 degrees. The result gave:

Mean wave direction = 23°
Significant wave height = 0.97 m (3.2 ft)
Wave period = 3.38 sec

Further computing using the ACES's Beta-Rayleigh Distribution, if we have our input at Energy based wave height, H_{m0} = 0.97 m, Peak spectral wave period, T_p = 3.38 sec, and water depth, d = 15 m, the output would be:

H_{rms} = 0.69 m
H_{med}: 0.57 m
$H_{1/3}$ = 0.97 m
$H_{1/10}$ = 1.23 m
$H_{1/100}$ = 1.61 m

4.2. Result 2 - Bretschneider Nomogram

The Bretschneider Nomogram (Bretschneider, 1970) was used to estimate waves based on wind fetch. The following parameters were assumed based on the largest average wind speed for the 2010-2012 CRVA2 wind record. From the wind speed of 18.2 m/s (35.4 knots) (Figure 8) and fetch length of 12.1 km (6.54 nautical miles), the resultant wave height was 5 ft (1.5 m), wave period of 5 sec, wind duration of 1.5 hours. An associated wave direction of 23 ° is assumed (from ACES computation).

Further computing these results using ACES, if we have our input at Energy based wave height, H_{m0} = 1.5 m, Peak spectral wave period, T_p = 5 sec, and water depth, d = 15 m, output would be:

H_{rms} = 1.06 m
H_{med}: 0.88 m
$H_{1/3}$ = 1.49 m
$H_{1/10}$ = 1.91 m
$H_{1/100}$ = 2.49 m

4.3. Wave period- Bretschneider

To estimate the critical wave period, $T_{1/100}$, an equation derived from JONSWAP (Hasselman et al., 1973)

$$T_p = 9.8U^{-1/3}H_{m0}^{2/3} \tag{10}$$

can be used where $H_{1/100}$ and $T_{1/100}$ would be substituted in place of H_{m0} and T_p. Equation 10 gives a good approximation when used for ACES and Bretschneider.

Here, it is used for Bretschneider $T_{1/100}$, where $H_{1/100}$ = 2.49 m and U=18.2m gives a result of $T_{1/100}$ = 6.84 sec.

4.4. Rayleigh distribution - Bretschneider

For the remainder of the report, only the results from the Bretschneider Nomogram, have been further examined since these values were considered the most conservative.

Figures 9 and 10 show the Rayleigh Distribution for Station CRVA2 for 2011 plotted in ACES (Fig 9) and in Matlab (Fig 10 – top panel). This is from the governing equation, Equation 2, which solves for $p(H)$ using the Bretschneider wave heights. The cumulative distribution function is also plotted in Matlab (Fig 10 – bottom panel) which is from Equation 3, solving for $P(H)$ using the Bretschneider wave heights.

Figure 11 shows the probability of exceedence for Station CRVA2 for 2011. This is from the governing equation, Equation 4, which solves for $Q(H)$ using the Bretschneider wave heights. Therefore, if the significant wave height is 1.5m, the height of the highest 1% of the waves $H_{1/100}$ would be 2.5m. Figure 11 also shows that $Q(H) = 0.135$ or 13.5% of the waves exceed the significant wave height.

4.5. Wave theory classification- Bretschneider

For wave classification, Figure 12 is used to illustrate the approximate limits of validity for wave theories (Le Mehaute, 1969) to determine whether the waves in this study were deep, transitional or shallow water waves, and what the appropriate Stokes analytical order was (i.e. second-order, third-order).

The wave period $T_{1/100}$ = 6.84 sec was used for wave theory classification (Table 2). Wave theory classification for Bretschneider results achieved in this study are presented here, where $H_{1/100}$ = 2.5m, with respective wave period, $T_{1/100}$ = 6.84sec and depth, d = 15m.

From Figure 12, the value d / gT^2 was used to classify the waves as deep, transitional, or shallow. Also from Figure 12, the value of H / gT^2 was used to classify the waves as Stokes' second-order, or Stokes' third-order. After classifying the order (e.g. Stokes' second order), wavelength L could be solved using Eqns. 7 or 9. For Stokes' second-order, $T_{1/100}$ and depth, d, were used to solve for wavelength, L_2 (Eqn. 9). After wavelength L was calculated, another check was performed to see if waves were deep, transitional, or shallow where d / L is estimated (Table 2). The result yielded that the critical wave should be considered a surface gravity wind wave in the transitional zone, governed by Stokes' second order wave theory.

5. Conclusion

With the limitations of one land-based wind station as the only reliable data source which only had 2 years of reliable data, assumptions needed to be made for this study that were reasonable. ACES, Bretschneider Nomogram, Rayleigh distribution, wave theory classification were the tools for describing the critical wind-waves found affecting Station CRVA2. From this study, the results yielded the following wave parameters with the probability of exceedence of $\leq$1%:

Critical wave height, $H_{1/100}$ = 2.5 meters

Critical wave period, $T_{1/100}$ = 6.8 seconds

Critical wave direction = 23°

These results are meant to guide the design of the pile-guided floating ferry landings that are located at latitude 60deg 33.431min N (i.e. 60.55718), and longitude 145deg 45.326min W (i.e. 145.75543W = 214.24457E).

6. References

ACES (1992). *Automated Coastal Engineering System Technical Reference.* Coastal Engineering Research Center, Waterways Exp. Station, Corps of Engineers, Vicksburg, MS

Airy, G.B. (1845). Tides and waves. *Encyc. Metrop.*, 192, 241–396.

Bretschneider, C.L. 1970. *Forecasting relations for wave generation*. Look Lab/ Hawaii, 1, No.3, University of Hawaii, USA, Aug 1970.

City of Cordova (2012) City of Cordova Alaska <http://www.cityofcordova.net>

CDFU (2012) *A historical narrative of fishing in the Prince William Sound/ Copper River Area.* Cordova District Fisherman United, http://www.cdfu.org, 28 November 2012.

Chamberlin, C. (2012) *A tsumani forecast model for Cordova, Alaska*. NOAA Center for Tsunami Research, Pacific Marine Environmental Laboratory.

Diebel J. and J. Norda (2013). *Weatherspark.* http://weatherspark.com

Hasselmann, K., T.P. Barnett, E. Bouws, H. Carlson, D.E. Cartwright, K. Enke, J.A. Ewing, H. Gienapp, D.E. Hasselmann, P. Kruseman, A. Meerburg, P. Müller, D.J. Olbers, K. Richter, W. Sell and H. Walden (1973). Measurements of wind-wave growth and swell decay during the Joint North Sea Wave Project (JONSWAP). *Deutsche Hydrographische Zeitschrift* A8 (12), 95pp.

Le Méhauté, B. (1969). An introduction to hydrodynamics and water waves. *ESSA Tech. Rep.* ERL 118-Pol 3-2.

Longuet-Higgins, M.S. (1952). On the Statistical Distribution of the Heights of Sea Waves, *J. Mar. Res.*, 11, 246-266.

Losada, I.J. and J.A. Revilla (2009). Applications to Fluid Mechanics: Water Wave Propagation, in Continuum Mechanics, (eds. Jose Merodio), in Encyclopedia of Life Support Systems (EOLSS), Developed under the Auspices of the UNESCO, Eolss Publishers, Oxford, UK, [http://www.eolss.net]

Mackline, S.A., G.M. Lackman, and J. Gray (1988). Offshore-directed wind in the vicinity of Prince William Sound, Alaska. *Monthly Weather Rev*. 116, 1289-1301.

Mesinger F., G. DiMego, et al. (2006). North Amercian Regional Reanalysis. Boulder, CO NOAA.OAR/ESRL PSD:42.

NOAA (2012a). *National Buoy Data Center.* <http://www.ndbc.noaa.gov>

NOAA (2012b). National Oceanic and Atmospheric Administration – *NOAA Nautical Chart, Catalog No. 16710*, Scale 1:30,000, Channel Island to Cordova <http://www.charts.noaa.gov/OnLineViewer/AlaskaViewerTable.shtml>

PIANC (1992). *Guidelines for the design and construction of flexible revetments incorporating geotextiles in marine environment*. PTC2 report of Working Group no. 21 – Supplement to Bulletin 78/79.

Smith, J.M. (1991). Wind-Wave Generation on Restricted Fetches," Miscellaneous Paper CERC-91 -2, US Army Engineer Waterways Experiment Station, Vicksburg, MS.

Sorensen, R.M. (1993). *Basic Wave Mechanics for Coastal and Ocean Engineers*. John Wiley & Sons, Inc. ISBN 0-471-55165-1. 284 pp.

Spies, R.B. (2007). *Long-term Ecological Change in the Northern Gulf of Alaska*. Elsevier Science, 1st Edition, 608 pp. ISBN 0444529608

SPM (1984). *Shore Protection Manual*. Vol. 2. Fourth edition. Coastal Engineering Research Center, Waterways Exp. Station, Corps of Engineers, Vicksburg, MS

Stokes G.G. (1847). On the theory of oscillatory waves. *Trans Cambridge Philos Soc*, 8, 441-473.

Thompson, E. F., and C.L. Vincent (1984). Shallow Water Wave Height Parameters. *Journal of Waterway, Port, Coastal and Ocean Engineering*, American Society of Civil Engineers, Vol. 110, No. 2, pp 293-299.

WMO (World Meteorological Organization) (1998). *Guide to Wave Analysis and Forecasting, Second Edition*. WMO-No. 702, Secretariat of the World Meteorological Organization – Geneva Switzerland. ISBN 92-63-12702-6. 159 pp.

WIS (2012). *Wave Information Studies (WIS)* <http://wis.usace.army.mil/hindcasts.shtml?dmn=atlWIS>

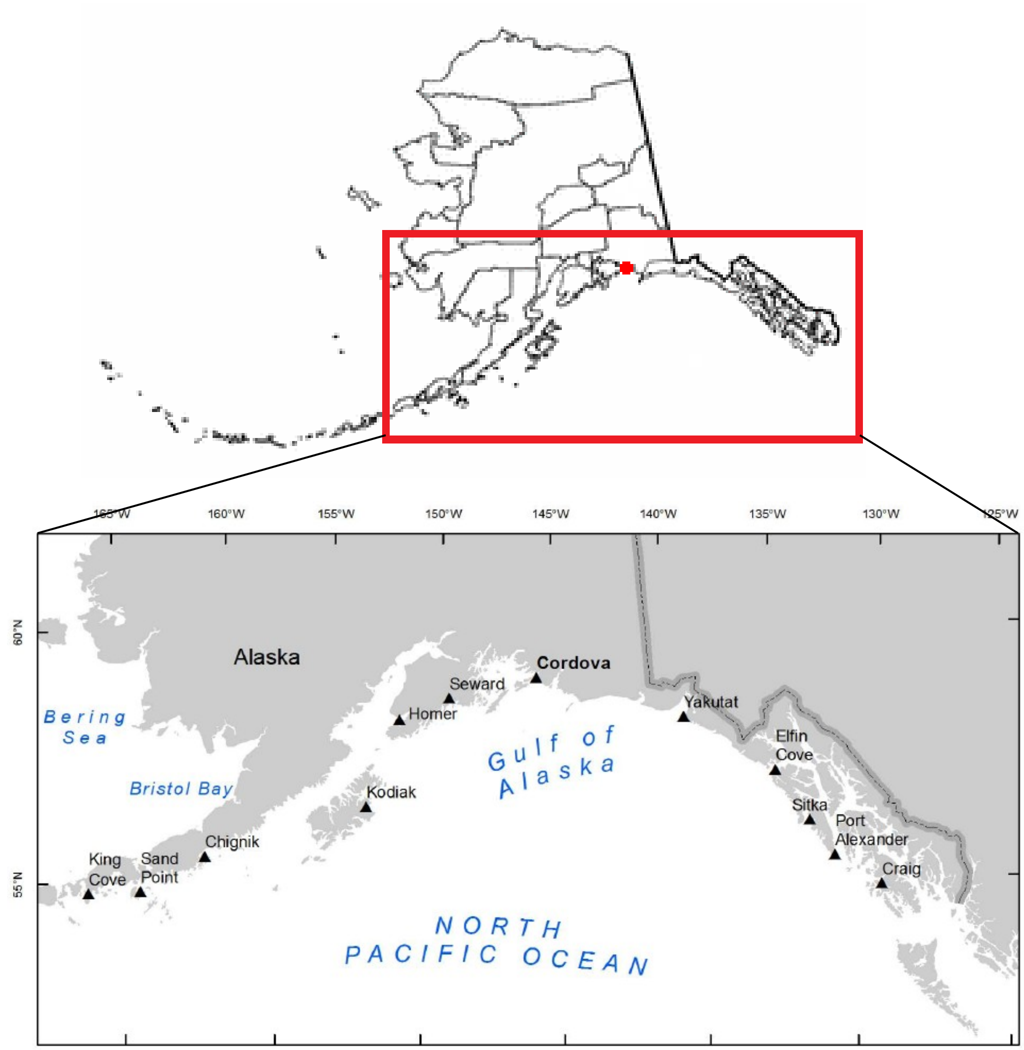

Figure 1: Alaska map (top) showing Cordova, Alaska (red dot) and Gulf of Alaska map inset (bottom).

Figure 2: Alaska map showing Cordova, Alaska (red rectangle). Note the sheltered inland location of Cordova.

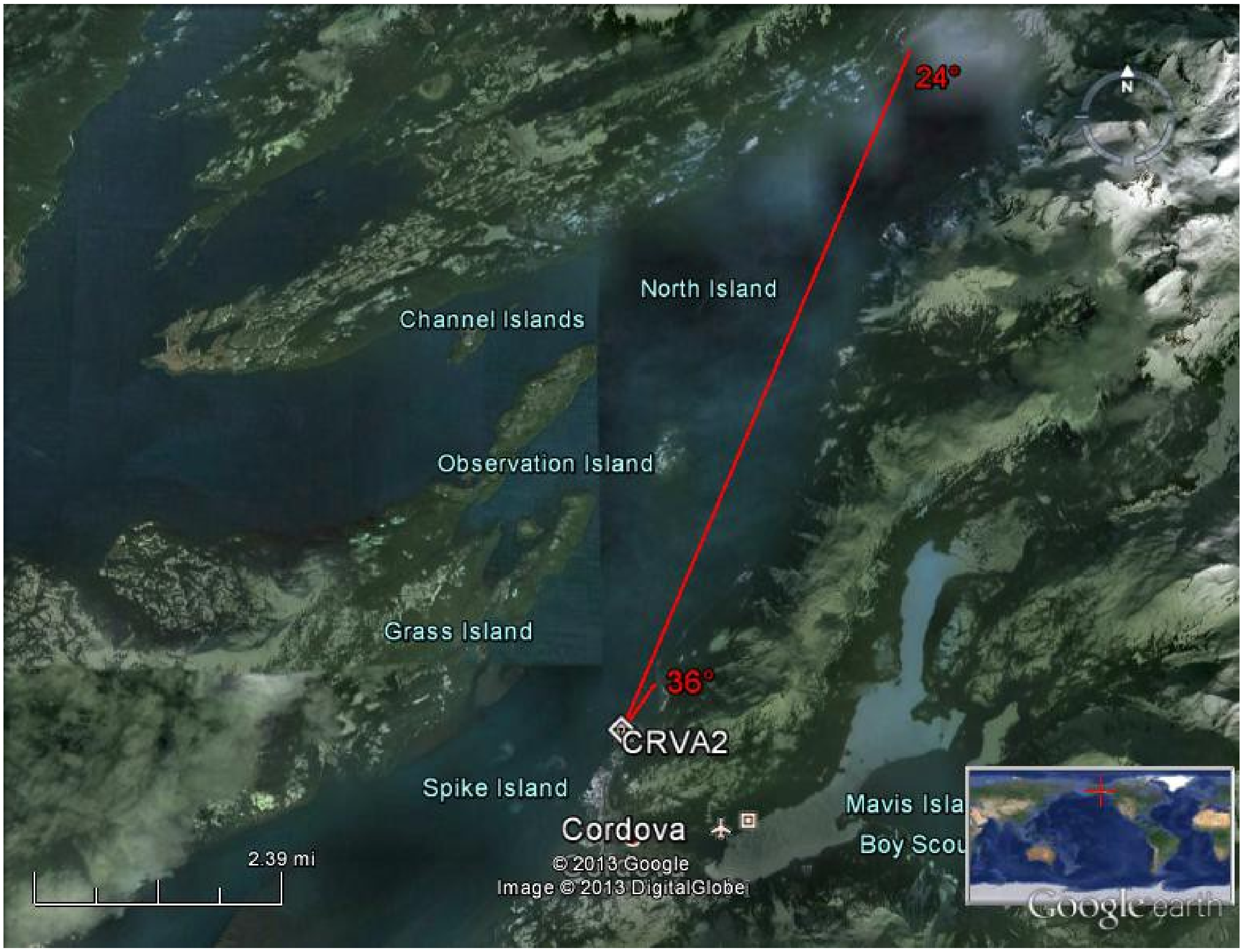

Figure 3: Fetch of two wind observations that contain the highest number of observations within the wind record set for Station CRVA2 for 2011.

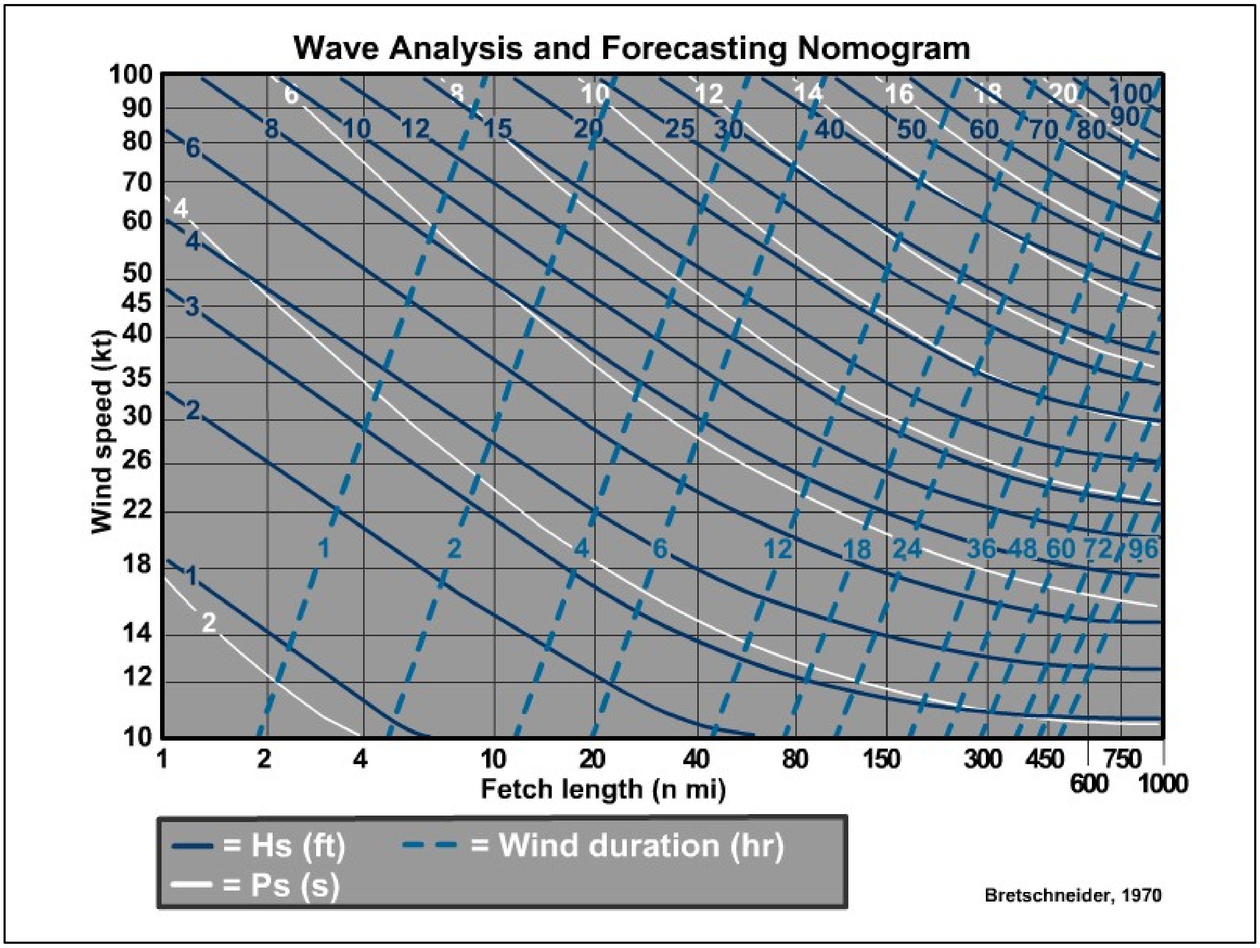

Figure 4: Wave analysis and forecasting Nomogram (Bretschneider, 1970)

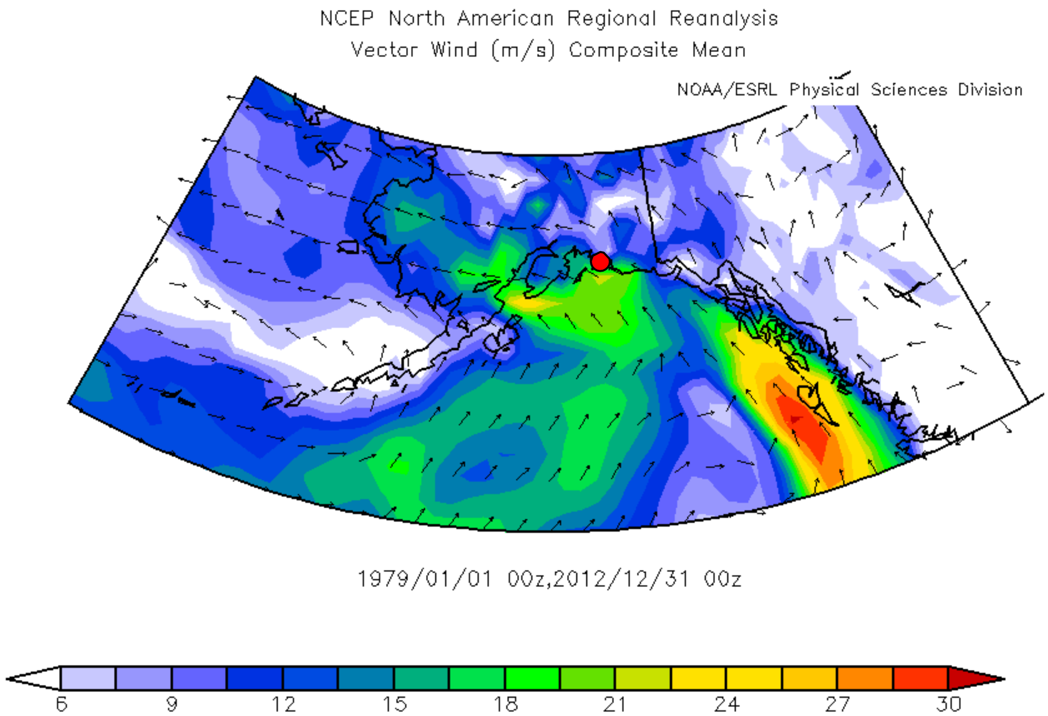

Figure 5: North American Regional Reanalysis (NARR) plot of vector winds at a 1° resolution at 925mb showing domain of lat 50 to 65N, and long 180 to 240E. Cordova shown (red dot).

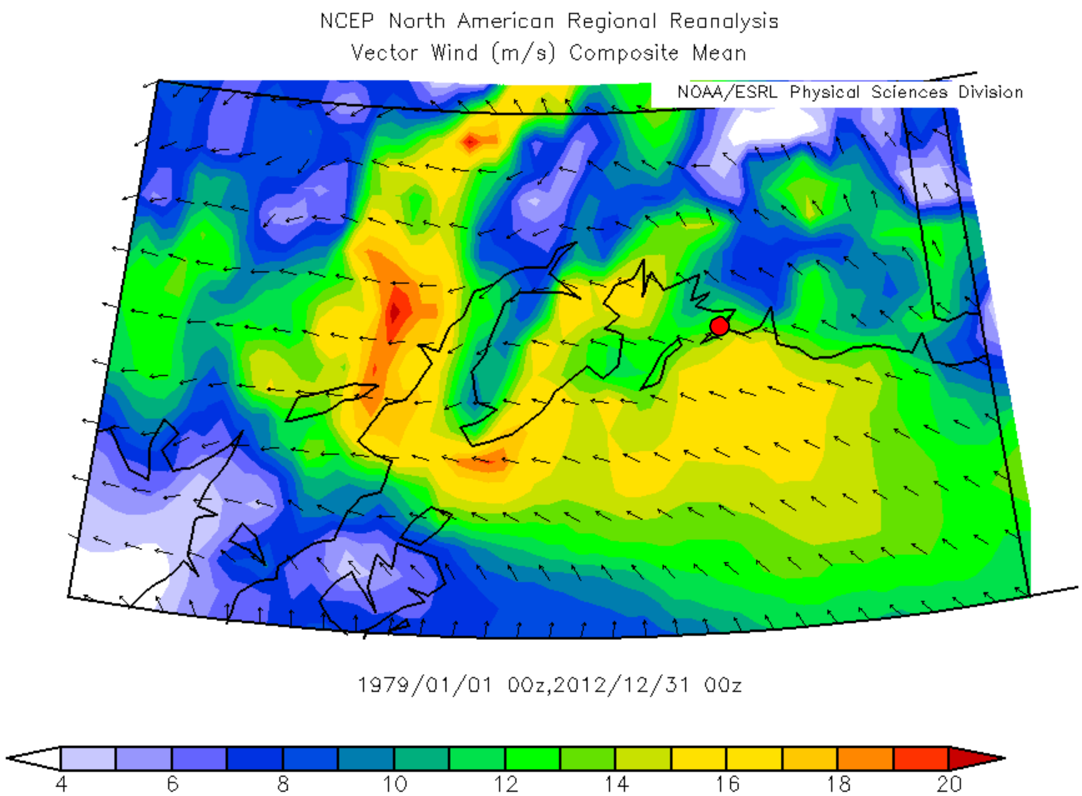

Figure 6: North American Regional Reanalysis (NARR) plot of vector winds at a 0.3° resolution at 1000mb showing domain of lat 57 to 63N, and long 200 to 220E. Cordova shown (red dot).

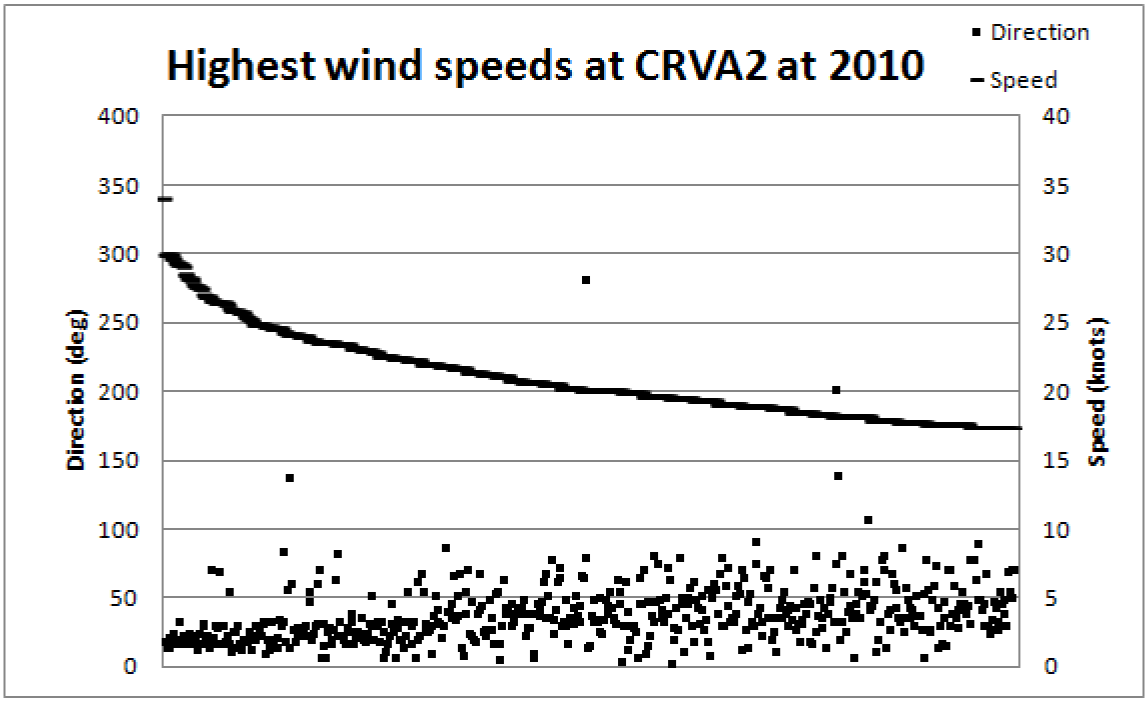

Figure 7: Highest wind speeds => 9 m/s (and their accompanying directions) at Station CRVA2 for the year 2010 encompassing 551 observations.

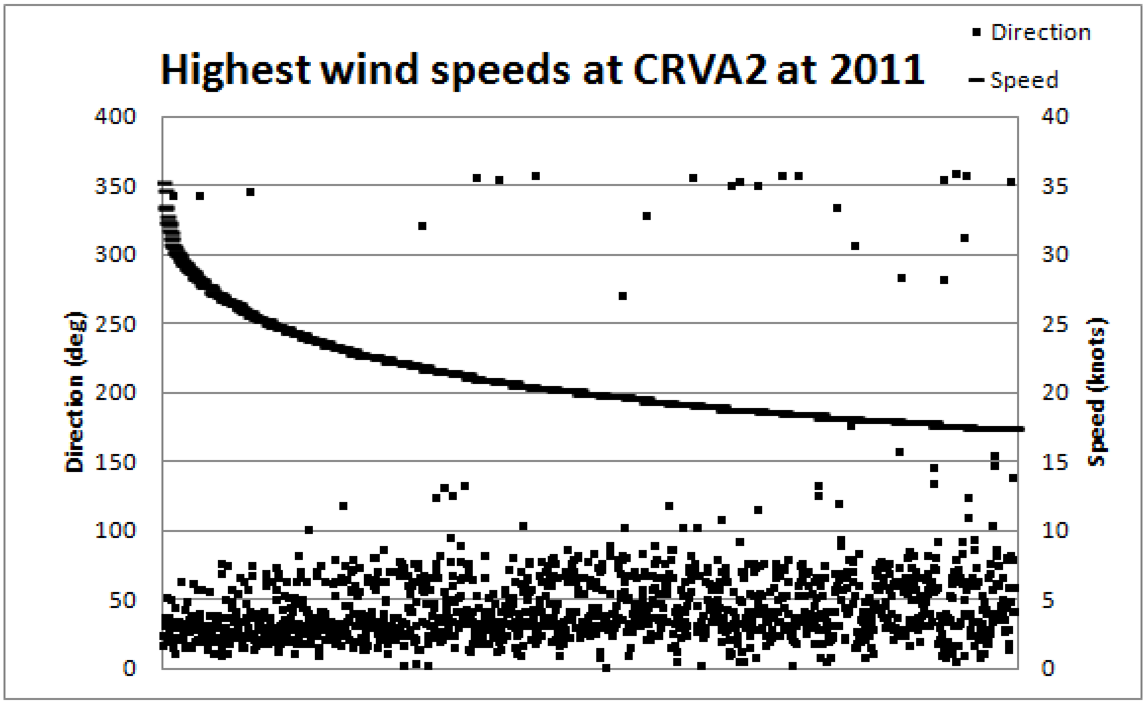

Figure 8: Highest wind speeds => 9 m/s (and their accompanying directions) at Station CRVA2 for the year 2011 encompassing 1400 observations.

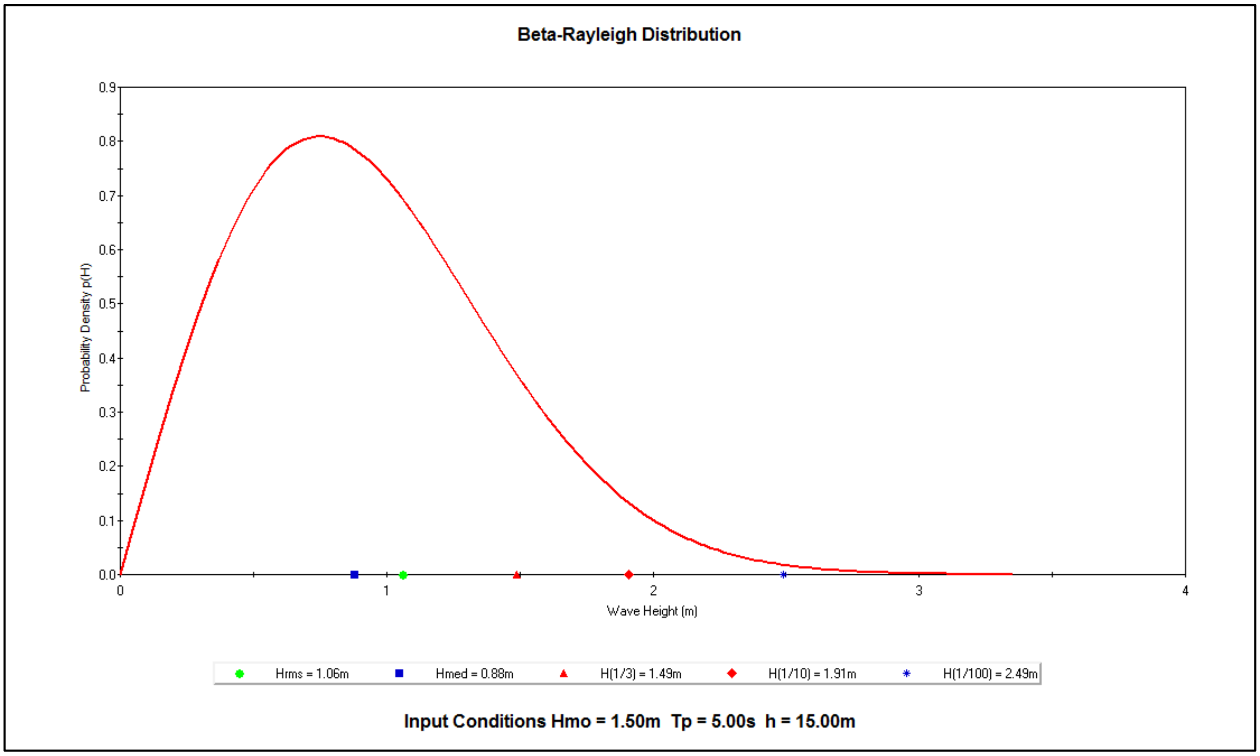

Figure 9: ACES Beta-Rayleigh Distribution for Bretschneider for CRVA2, 2011

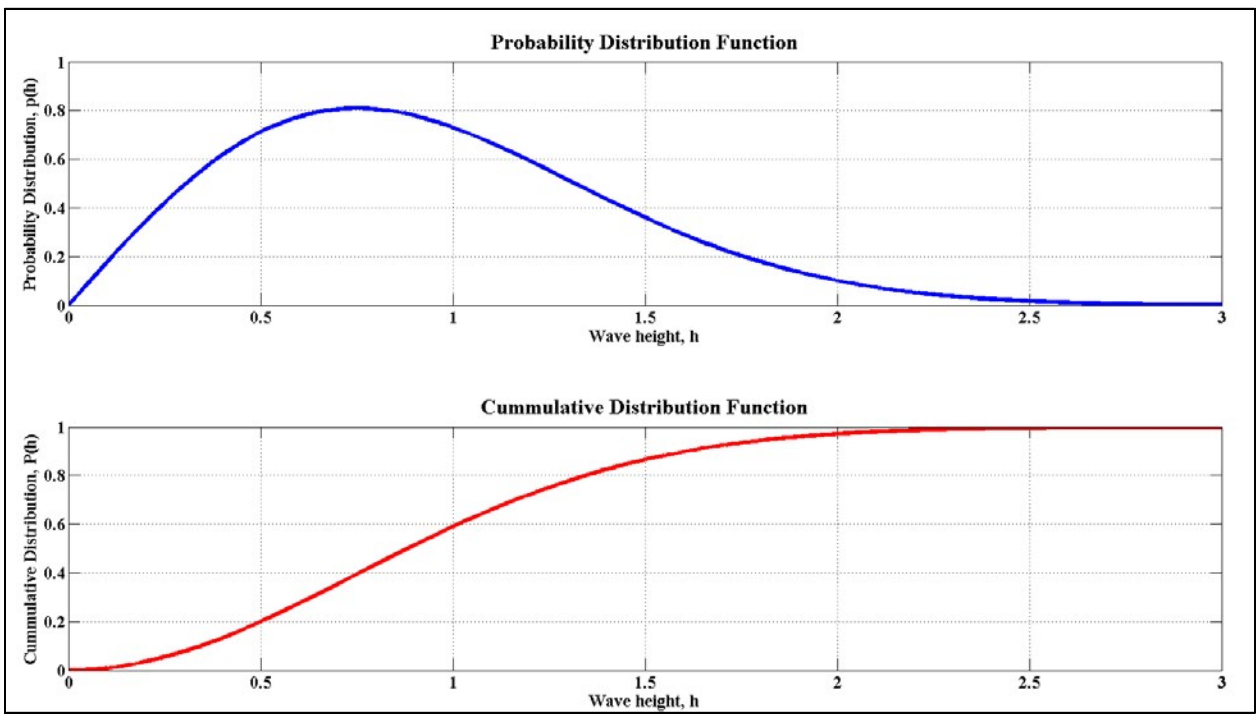

Figure 10: Rayleigh Distribution for Bretschneider for CRVA2, 2011

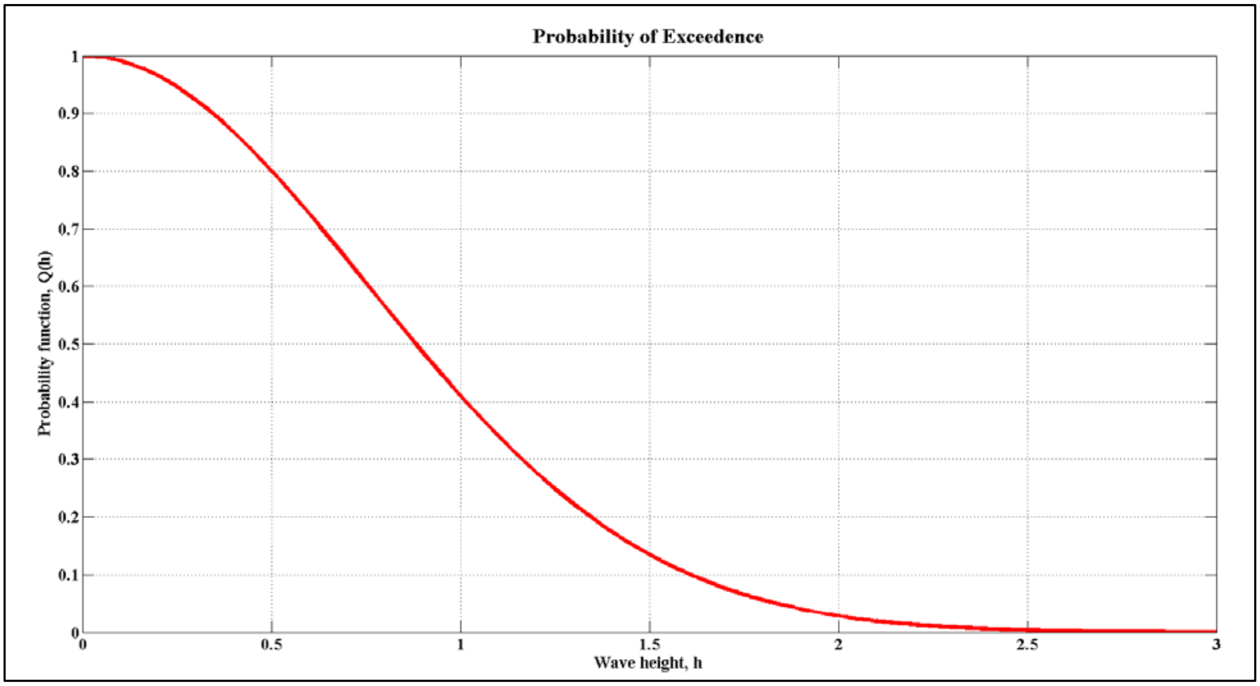

Figure 11: Probability of Exceedence for Bretschneider for CRVA2, 2011

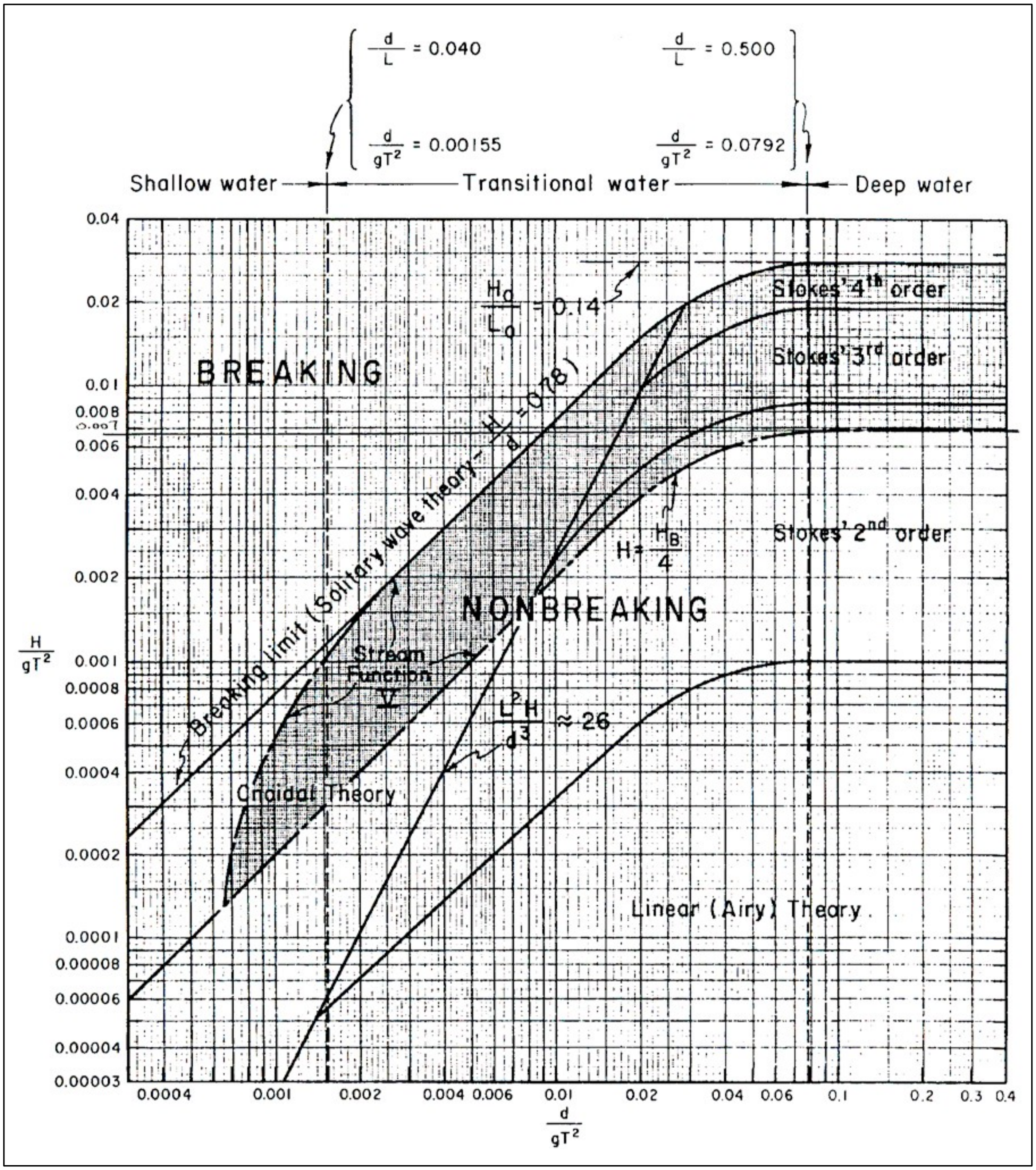

Figure 12: Wave theory limits. Approximate limits for various wave theories. Le Mehaute (1969).

Table 1. ACES fetch adjustment results, Station CRVA2 for 2011

Station CRVA2								
Radial number	**Fetch Angle Measured**	**Fetch Angle Encompasses**	**No. obs.**	**Fetch Length (km)**	**Fetch Length (nautical miles)**	**Wind Speed (m/s)**	**Wind Speed (knots)**	**Wave Height (ft)**
1	0	355-6 deg	19	8.23	4.45	9.98	19.40	2.5
2	12	7-18 deg	93	4.07	2.2	11.12	21.61	< 2
3	24	19-30 deg	336	12.1	6.54	11.41	22.18	3.2
4	36	31-42 deg	376	0.97	0.52	10.91	21.22	<< 2
5	48	43-54 deg	138	0.85	0.46	10.51	20.43	<< 2
6	60	55-66 deg	184	0.67	0.36	10.41	20.23	<< 2
7	72	67-78 deg	154	0.21	0.12	10.33	20.08	<< 2
8	84	79-90 deg	51	0.07	0.04	10.05	19.55	<< 2
9	96	91-354 deg	47	-	-	10.11	19.65	-

Table 2. Wave theory classification for Bretschneider results where $H_{1/100}$ = 2.5m, with respective wave period, $T_{1/100}$ = 6.84sec and depth, *d*=15m.

Category	H1/100 = 2.5m, d=15m
T1/100 (sec)	6.84
d/gT^2	0.032682
Wave classification for d/gT^2	transitional
H/gT^2	0.00545
Order	Stoke's 2nd
L (m)	65.32
d/L (m/m)	0.230
Wave classification for d/L	transitional

Table 3. Classification of gravity waves. Classification of gravity waves by water depth. From US Army Shore Protection Manual (1984).

Classification	d/L	$2\pi d/L$	**tanh** $(2\pi d/L)$
Deep water	> 1/2	$> \pi$	≈ 1
Transitional	1/25 to1/2	1/4 to π	tanh $(2\pi d/L)$
Shallow water	< 1/25	< 1/4	$\approx 2\pi d/L$